Unified Inverse Dynamics of Modular Serial Mechanical Systems with Application to Soft Robotics

Pietro Pustina[1,2], Cosimo Della Santina[2,3], Alessandro De Luca[1]

***Abstract*—The robotic field has been witnessing a progressive departure from classic robotic systems composed of serial/stiff links interconnected by simple rigid joints. Novel robotic concepts, e.g., soft robots, often maintain a series-like structure, but their mechanical modules exhibit complex and unconventional articulation patterns. Research in efficient recursive formulations of the dynamic models for subclasses of these systems has been extremely active in the past decade. Yet, as of today, no single recursive inverse dynamics algorithm can describe the behavior of all these systems. This paper addresses this challenge by proposing a new iterative formulation based on Kane equations. Its computational complexity is optimal, i.e., linear with the number of modules. While the proposed formulation is not claimed to be necessarily more efficient than state-of-the-art techniques for specific subclasses of robots, we illustrate its usefulness in the modeling of different complex systems. We propose two new models of soft robots: (i) a class of pneumatically actuated soft arms that deform along their cross-sectional area, and (ii) a piecewise strain model with Gaussian functions.**

Note: This paper has supplementary material that can be accessed at the following link: https://drive.google.com/drive/folders/13wwUjjX7jm1VkRfYzafbWKtey3qWZ1_a?usp=sharing. The MATLAB code implementing the proposed algorithms can be found at the following link: https://github.com/piepustina/Jelly.

I. Introduction

In recent years, serial robotic systems have undergone a remarkable transformation, evolving from assemblies of rigid links and joints to articulated mechanical architectures built from complex modules. These include serial interconnections of parallel mechanisms [1], flexible link and joint manipulators [2], robots made of meta-materials [3], [4], continuum and soft arms [5]–[9], bio-hybrid robots [10]–[12], and rigid robots manipulating deformable objects [13]. In these systems, the range of admissible motions does not solely stem from the joints (if any), as in conventional rigid robots. In fact, it also arises from compliant and deformable elements like springs, variable stiffness actuators [14], and flexible and soft bodies [15]. Consequently, their joints and bodies can be conceptualized as mechanical modules providing degrees of freedom (DoF) to the system, as illustrated in Fig. 1. When the

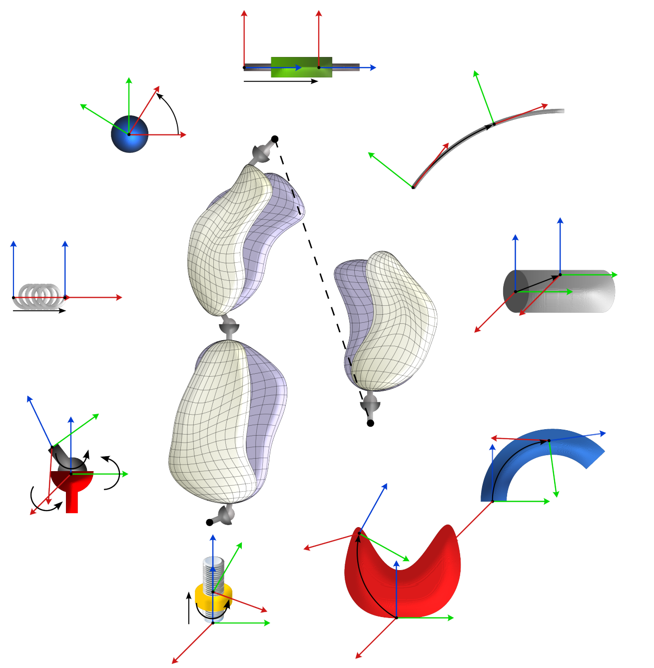

Figure 1: Selection of mechanical modules, i.e., joints and bodies, that can be used to assemble the class of robots considered in this work. Soft, hybrid, and bio-hybrid robots all fall into the class of robots that can be modeled this way. These bodies include but are not limited to possibly flexible joints (helical, spherical, elastic, rotational, and prismatic), beams, generic rigid bodies, and highly deformable bodies (1D, 2D, and 3D). The only requirement is that the motion of these components can be described, or approximated, by a finite set of configuration variables.

relative motion of each module is described, or approximated, by a finite set of configuration variables, the dynamics follows the principles of Lagrangian mechanics and is described by ordinary differential equations of the form

$$\boldsymbol{M}(\boldsymbol{q})\ddot{\boldsymbol{q}} + \boldsymbol{n}(\boldsymbol{q},\dot{\boldsymbol{q}}) = \boldsymbol{Q}(\boldsymbol{q},\dot{\boldsymbol{q}},\boldsymbol{u}), \tag{1}$$

where $\boldsymbol{q} \in \boldsymbol{\mathcal{M}} \subseteq \mathbb{R}^n$ is the configuration vector, with $\dot{\boldsymbol{q}}$ and $\ddot{\boldsymbol{q}}$ its time derivatives, and $\boldsymbol{u} \in \mathbb{R}^m$ groups the inputs to the system. Furthermore, $\boldsymbol{M}(\boldsymbol{q}) \in \mathbb{R}^{n\times n}$ denotes the inertia matrix, $\boldsymbol{n}(\boldsymbol{q},\dot{\boldsymbol{q}})$ collects Coriolis and centrifugal terms, and $\boldsymbol{Q}(\boldsymbol{q},\dot{\boldsymbol{q}},\boldsymbol{u})$ models active forces, both conservative and non-conservative, such as the gravitational force, stress and actuator inputs.

The forward dynamic problem (FDP) for (1) consists in computing $\ddot{\boldsymbol{q}}$ from $\boldsymbol{q}$, $\dot{\boldsymbol{q}}$ and $\boldsymbol{u}$. The FDP finds its main

[1]Department of Computer, Control and Management Engineering, Sapienza University of Rome, Rome, Italy. pustina@diag.uniroma1.it, deluca@diag.uniroma1.it

[2]Department of Cognitive Robotics, Delft University of Technology, Delft, Netherlands. c.dellasantina@tudelft.nl

[3]Institute of Robotics and Mechatronics, German Aerospace Center (DLR), Oberpfaffenhofen, Germany.

application in simulation to assess the system behavior across different conditions. While the FDP has been completely solved for rigid-bodied systems [16], it remains an open problem for generic mechanical systems, including among others systems with deformable bodies. Historically, researchers have focused on attacking this challenge under small deformations[1]. Despite early seminal works from the 80's [17], the topic continues nowadays to be an active field of research [18], [19]. However, these techniques are not applicable nor directly generalizable to most of the systems we discussed above, as they often violate the small-deformations hypothesis. An example of such systems that we will focus our attention on in the rest of this paper is continuum soft robots [20]–[23].

The dual problem of identifying the active forces responsible for a given acceleration, i.e., the inverse dynamics problem (IDP), has received significantly less attention. However, the IDP plays a pivotal role in various applications that are crucial for the advancement of autonomous and intelligent robotic systems, including real-time control [23]–[25], system identification [26], trajectory generation [27] and optimization [28], [29], and mechanical design [30], [31]. In this context, the computation time becomes essential, especially when the dynamics has numerous DoF. Furthermore, it is noteworthy that a procedure for the IDP can also be used to solve - efficiently although not optimally - the FDP [16].

Numerous studies have explored the computation of the IDP for flexible link robots using different approaches. These include the Euler-Lagrange (EL) method [32]–[35], the generalized Newton-Euler (NE) equations [36]–[38], the Gibb-Appell equations [39], and the Kane equations [40]–[42]. Again, all the mentioned works share three main assumptions: (i) small deflections, (ii) slender bodies and (iii) the ability to separate rigid and deformable motion. Unfortunately, such hypotheses are seldom verified when high deformation occurs, limiting the application of previous approaches to deformable systems. Assumptions (i) and (iii) have been partially relaxed, but not removed, in the context of soft robotics for reduced order models (RoM) of 1D continua. In particular, [20] proposes an ID procedure for slender continuum soft robots with piecewise constant strain (PCS). The method has been extended in [43] to encompass various kinematic models and rigid bodies. In addition, [23] removed the PCS hypothesis in place of a modal Ritz reduction of the strain. Still, these works are limited to thin bodies (hypothesis (ii)) and assume a linear separation between material and generalized coordinates, i.e., the strain $\boldsymbol{\xi} \in \mathbb{R}^6$ can be expressed as $\boldsymbol{\xi} = \boldsymbol{\Phi}(s)\boldsymbol{q}$, being s and $\boldsymbol{q}$ the material and generalized coordinates, respectively.

This work aims to take a step further by proposing a method that has the benefit of eliminating such remaining limiting assumptions. The only hypothesis is that the configuration space of the system can be described by a finite-dimensional model. In our approach, kinematics is treated as input to the procedure rather than pre-existing information. In particular, the robot is seen as an assembly of complex modules, its joints and bodies, whose relative motion is parameterized by an abstract set of material and configuration variables. This way, it is possible to obtain a unified approach to recursively solve the IDP for serial multibody mechanical systems, comprising both rigid and deformable bodies, and remove any assumption regarding their kinematic model. Each body can have lumped or distributed mass with a three-dimensional domain. The framework also applies to systems comprising modules obtained from novel 3D reduced-order models [44], where the deformations are expressed using function composition. Fig. 1 shows a collection of some modules that the proposed method can handle. To the best of our knowledge, the IDP has never been tackled in such a general setting. This is likely due to the recent proliferation of robots, especially those developed by the soft robotics community, that cannot be modeled as assemblies of rigid or flexible bodies.

In analogy with the recursive Newton-Euler approach for rigid systems, the method has linear complexity in the number of bodies. It consists of two steps, namely a forward propagation that initiates velocities and accelerations from the base, followed by the computation of the generalized active forces in a backward step. The approach has its foundations in the Kane equations [45], [46], a choice motivated by their intermediary nature between the EL and NE equations. In view of their equivalence with the EL method, the obtained equations of motion (EoM) can be viewed as a recursive form of the EL formulation and a generalization to the seminal results of [32], [47]. In these works, a recursive form of EL equations with linear complexity has been derived for serial rigid [47] and flexible link robots [32].

The main contributions of the paper are summarized in the following.

1) We provide a general definition for the configuration space of serial modular robotic systems, encompassing both rigid and deformable bodies.
2) By using the Kane equations, we prove a recursive formulation of the EoM. Considering the equivalence between the EL and Kane equations, the method can be seen as a recursive representation of the EL equations.
3) We derive algorithms solving the IDP for the evaluation of the generalized active forces and of the actuation forces. In both cases, the computational complexity grows linearly with the number of bodies.

To show the generality of the approach, the findings are supported by simulations results on two new RoM of continuum soft robots. First, we consider a pneumatically actuated soft robot and model the radial deformation due to air pressure change in the actuation chambers. In a second simulation, taking inspiration from [48], we use Gaussian distributions to model the strain of a tentacle-like soft arm. Additional simulations of state-of-the-art multibody mechanical systems can be found in the supplementary material [49].

A. Notation

We denote vectors and matrices with bold letters. Arguments of the functions are omitted when clear from the context. Table I presents the notation adopted in the paper.

[1]Usually referred to as flexibility.

Table I: Nomenclature

Symbol	Description
$\mathbb{R}^n$	Euclidean space of dimension n
$\mathbb{R}^{n\times m}$	Space of $n \times m$ matrices over $\mathbb{R}$
$SE(3)$	Special Euclidean group of dimension 3
$so(3)$	Special orthogonal algebra of dimension 3
$\boldsymbol{I}_n \in \mathbb{R}^{n\times n}$	Identity matrix of dimension n
$\boldsymbol{0}_{n\times m} \in \mathbb{R}^{n\times m}$	Matrix of zeros
$\boldsymbol{1}_n \in \mathbb{R}^n$	Column vector of ones
$\boldsymbol{S}_i \in \mathbb{R}^n$	Column i of matrix $\boldsymbol{S} \in \mathbb{R}^{n\times m}$
$S_{ij} \in \mathbb{R}$	Element in row i and column j of $\boldsymbol{S}$
$\tilde{\boldsymbol{r}} \in so(3)$	Skew symmetric matrix defined by $\boldsymbol{r} \in \mathbb{R}^3$
$\boldsymbol{A}^\vee \in \mathbb{R}^3$	Euclidean vector associated with $\boldsymbol{A} \in so(3)$
$\boldsymbol{A}^T \in \mathbb{R}^{m\times n}$	Transpose of $\boldsymbol{A} \in \mathbb{R}^{n\times m}$
$\boldsymbol{AB} \in \mathbb{R}^{m\times p}$	Matrix multiplication of $\boldsymbol{A} \in \mathbb{R}^{m\times n}$ and $\boldsymbol{B} \in \mathbb{R}^{n\times p}$
$\boldsymbol{A} \otimes \boldsymbol{B} \in \mathbb{R}^{pm\times qn}$	Kronecker product of $\boldsymbol{A} \in \mathbb{R}^{m\times n}$ and $\boldsymbol{B} \in \mathbb{R}^{p\times q}$
$\mathrm{vec}(\boldsymbol{A}) \in \mathbb{R}^{mn}$	Vectorization of $\boldsymbol{A} \in \mathbb{R}^{m\times n}$
$\boldsymbol{a} \times \boldsymbol{b} = \tilde{\boldsymbol{a}}\boldsymbol{b} \in \mathbb{R}^3$	Cross product of $\boldsymbol{a} \in \mathbb{R}^3$ and $\boldsymbol{b} \in \mathbb{R}^3$
$\nabla_{\boldsymbol{x}} f \in \mathbb{R}^h$	Gradient of $f \in \mathbb{R}$ with respect to $\boldsymbol{x} \in \mathbb{R}^h$
$\nabla_{\boldsymbol{x}} \boldsymbol{f} \in \mathbb{R}^{h\times l}$	Jacobian transpose of $\boldsymbol{f} \in \mathbb{R}^l$ with respect to $\boldsymbol{x} \in \mathbb{R}^h$
$\nabla_{\boldsymbol{x}} \cdot$	Divergence operator in coordinates $\boldsymbol{x} \in \mathbb{R}^h$

B. Structure of the paper

The rest of the paper is organized as follows. In Section II, we establish the configuration space that characterizes the considered class of systems. Herein, we derive both the direct kinematics and the first and second-order differential kinematics. Section III introduces the Kane equations for the system. A recursive form for these equations is proven in Section IV, offering immediate utility in assessing generalized active forces. In Section V, we expand the active forces to derive an ID recursive procedure for evaluating the actuation forces only. Section VI presents simulations results, and Section VII concludes the paper.

II. Kinematics

As a first step towards solving the IDP, in this section we characterize configuration space of a generic serial modular mechanical system. We then derive the forward kinematics and differentiate it with respect to time to obtain the first and second-order differential kinematics.

Consider a holonomic serial chain with a fixed base of N bodies $\mathcal{B}_i$, each one connected to its predecessor by a joint $\mathcal{J}_i$; $i \in \{1, \cdots, N\}$, as shown in Fig. 2. To describe the kinematics, it is needed to introduce two types of configuration spaces: one for the joints and another for the bodies. The former describes the relative motions between adjacent bodies, as in the case of rigid systems. Conversely, the latter captures the configurations a body can assume due to its deformability, if any.

Specifically, we define the configuration space of joint $\mathcal{J}_i$ at time t as follows

$$\mathcal{C}_{\mathcal{J}_i}(t) = \{(\boldsymbol{R}(t), \boldsymbol{p}(t)) \in \bar{V}_i(t)\},$$

where $\bar{V}_i(t) \subset SE(3)$ denotes the oriented volume occupied by $\mathcal{B}_i$ at t, assuming no internal deformations. Note that this definition encompasses solely the relative motions of the bodies due to the joints. As for rigid systems, $\mathcal{C}_{\mathcal{J}_i}$ is described by a set of generalized coordinates $\boldsymbol{q}_{\mathcal{J}_i}(t)$, and its dimension cannot exceed six, i.e., $\dim(\mathcal{C}_{\mathcal{J}_i}) = \dim(\boldsymbol{q}_{\mathcal{J}_i}) = n_{\mathcal{J}_i} \leq 6$, with the limit cases $\mathcal{C}_{\mathcal{J}_i} = \varnothing$ and $\mathcal{C}_{\mathcal{J}_i} = SE(3)$ corresponding to a fixed and free moving body, respectively.

The above definition does not account for deformations, so motivating the introduction of the body configuration space. The configuration space of $\mathcal{B}_i$ at time t is

$$\mathcal{C}_{\mathcal{B}_i}(t) = \{(\boldsymbol{R}(t), \boldsymbol{p}(t)) \in (\tilde{V}_i(t) - \bar{V}_i(t))\},$$

where $\tilde{V}_i(t) \subset SE(3)$ corresponds to the oriented region of space occupied by $\mathcal{B}_i$. The set $\mathcal{C}_{\mathcal{B}_i}$ describes those configurations not represented by $C_{\mathcal{J}_i}$ because of deformability. Theoretically, $C_{\mathcal{B}_i}$ requires infinite configuration variables to be described. Instead, we assume that it can be parameterized by a minimal set of generalized coordinates $\boldsymbol{q}_{\mathcal{B}_i}(t)$ and material coordinates $\boldsymbol{s}_i \in V_i$, being V_i the volume in the reference configuration. This way, the number of coordinates $\boldsymbol{q}_{\mathcal{B}_i}$ defines the dimension of the configuration space, i.e., $\dim(\mathcal{C}_{\mathcal{B}_i}) = \dim(\boldsymbol{q}_{\mathcal{B}_i}) = n_{\mathcal{B}_i}$. For example, if $\mathcal{B}_i$ is rigid, then $\boldsymbol{q}_{\mathcal{B}_i} \in \varnothing$ because, by definition, in a rigid body, no internal deformations occur. Differently, for a slender continuum modeled under the piecewise constant curvature (PCC) hypothesis [50], $\boldsymbol{q}_{\mathcal{B}_i} \in \mathbb{R}^2$ and its components correspond to the curvatures along the x and y directions.

Remark 1. *We intentionally refrain from any assumption on how the body deformations can be described. This allows considering the IDP independently of the kinematic model of the system.*

In the following, we consider $\boldsymbol{q}_{\mathcal{J}_i}$ and $\boldsymbol{q}_{\mathcal{B}_i}$ as Euclidean vectors, i.e., $\boldsymbol{q}_{\mathcal{J}_i} \in \mathbb{R}^{n_{\mathcal{J}_i}}$ and $\boldsymbol{q}_{\mathcal{B}_i} \in \mathbb{R}^{n_{\mathcal{B}_i}}$. Despite this not being the case in many situations, e.g., for rigid robots with revolute joints, it does not constitute a problem for this paper since the focus its on computational methods. We also define the vectors

$$\boldsymbol{q}_i = \begin{pmatrix} \boldsymbol{q}_{\mathcal{J}_i} \\ \boldsymbol{q}_{\mathcal{B}_i} \end{pmatrix} \in \mathbb{R}^{n_i},$$

with $n_i = n_{\mathcal{B}_i} + n_{\mathcal{J}_i}$, and

$$\boldsymbol{q} = \begin{pmatrix} \boldsymbol{q}_1 \\ \vdots \\ \boldsymbol{q}_N \end{pmatrix} \in \mathbb{R}^n,$$

with $n = \sum_{i=1}^N n_i$, which group the generalized coordinates of each body and the entire system, respectively. Since $\mathcal{C}_{\mathcal{B}_i}$ and $\mathcal{C}_{\mathcal{J}_i}$ are completely specified by $\boldsymbol{q}_i$, the knowledge of $\boldsymbol{q}_i$ and of its time derivatives provides all the information required to describe the configuration space of the system at any instant of time, i.e.,

$$\mathcal{C}(t) = (\mathcal{C}_{\mathcal{J}_1}(t) + \mathcal{C}_{\mathcal{B}_1}(t)) \times \cdots \times (\mathcal{C}_{\mathcal{J}_N}(t) + \mathcal{C}_{\mathcal{B}_N}(t)) .$$

To compute the kinematics, we attach a reference frame to each particle [2] of $\mathcal{B}_i$ and at the distal end of $\mathcal{J}_i$, labeled as $\{S_{\mathcal{B}_i}(\boldsymbol{s}_i)\}$ and $\{S_{\mathcal{J}_i}\}$, respectively. We also denote with $\{S_i\}$ the reference frame of $\mathcal{B}_i$ associated to the point $\boldsymbol{s}_{\mathcal{J}_{i+1}} \in \mathcal{B}_i$ to which $\mathcal{J}_{i+1}$ is connected, i.e., $\{S_i\} = \{S_{\mathcal{B}_i}(\boldsymbol{s}_{\mathcal{J}_{i+1}})\}; i = \{1, \cdots, N-1\}$. For the last body, $\{S_N\}$ is the reference frame of an arbitrary point of the body. In addition, an inertial reference frame $\{S_0\}$ is assigned to the base. Recalling that $\mathcal{C}_{\mathcal{J}_i}$ and $\mathcal{C}_{\mathcal{B}_i}$ have finite dimension the following result holds.

Proposition 1. *For all joints $\mathcal{J}_i$ and bodies $\mathcal{B}_i; i \in \{1, \cdots, N\}$, of the system, there exist*

$$^{\mathcal{B}_{i-1}}\boldsymbol{T}_{\mathcal{J}_i}\left(\boldsymbol{q}_{\mathcal{J}_i}\right) = \begin{pmatrix} ^{\mathcal{B}_{i-1}}\boldsymbol{R}_{\mathcal{J}_i}\left(\boldsymbol{q}_{\mathcal{J}_i}\right) & ^{\mathcal{B}_{i-1}}\boldsymbol{t}_{\mathcal{J}_i}\left(\boldsymbol{q}_{\mathcal{J}_i}\right) \\ \boldsymbol{0}_{1\times 3} & 1 \end{pmatrix}, \quad (2)$$

and

$$^{\mathcal{J}_i}\boldsymbol{T}_{\mathcal{B}_i}\left(\boldsymbol{q}_{\mathcal{B}_i}, \boldsymbol{s}_i\right) = \begin{pmatrix} ^{\mathcal{J}_i}\boldsymbol{R}_{\mathcal{B}_i}\left(\boldsymbol{q}_{\mathcal{B}_i}, \boldsymbol{s}_i\right) & ^{\mathcal{J}_i}\boldsymbol{t}_{\mathcal{B}_i}\left(\boldsymbol{q}_{\mathcal{B}_i}, \boldsymbol{s}_i\right) \\ \boldsymbol{0}_{1\times 3} & 1 \end{pmatrix}, \quad (3)$$

where $^{\mathcal{B}_{i-1}}\boldsymbol{T}_{\mathcal{J}_i}\left(\boldsymbol{q}_{\mathcal{J}_i}\right)$ and $^{\mathcal{J}_i}\boldsymbol{T}_{\mathcal{B}_i}\left(\boldsymbol{q}_{\mathcal{B}_i}, \boldsymbol{s}_i\right)$ are the homogeneous transformation matrices from $\{S_{\mathcal{J}_i}\}$ to $\{S_{i-1}\}$ and from $\{S_{\mathcal{B}_i}(\boldsymbol{s}_i)\}$ to $\{S_{\mathcal{J}_i}\}$, respectively.

Note that $^{\mathcal{B}_{i-1}}\boldsymbol{T}_{\mathcal{J}_i}\left(\boldsymbol{q}_{\mathcal{J}_i}\right)$ remains independent of $\boldsymbol{s}_i$ since it describes the relative motion of two bodies induced by the joint. Conversely, $^{\mathcal{J}_i}\boldsymbol{T}_{\mathcal{B}_i}\left(\boldsymbol{q}_{\mathcal{B}_i}, \boldsymbol{s}_i\right)$ depend on $\boldsymbol{q}_{\mathcal{B}_i}$, which parameterizes the internal deformations of $\mathcal{B}_i$, and on $\boldsymbol{s}_i$ which acts as a label for the points of $\mathcal{B}_i$. In the case of rigid bodies, $^{\mathcal{J}_i}\boldsymbol{T}_{\mathcal{B}_i}$ does not depend on $\boldsymbol{q}_{\mathcal{B}_i}$ but only on $\boldsymbol{s}_i$. The above matrices are part of the known input data because they come from the configuration space of $\mathcal{B}_i$ and $\mathcal{J}_i$, both known by assumption. Without loss of generality, it is considered that the reference configuration is represented by $\boldsymbol{q}_{\mathcal{B}_i} = \boldsymbol{0}_{n_{\mathcal{B}_i}}$ so that $^{\mathcal{J}_i}\boldsymbol{T}_{\mathcal{B}_i}\left(\boldsymbol{0}_{n_{\mathcal{B}_i}}, \boldsymbol{s}_i\right)$ describes the volume occupied by $\mathcal{B}_i$ in the reference configuration, see Fig. 2. In Fig. 3, we also show examples of the above transformations to clarify this aspect further. Given (2)–(3), it is possible to compute the relative transformation between two adjacent bodies, defined as

$$^{\mathcal{B}_{i-1}}\boldsymbol{T}_{\mathcal{B}_i}(\boldsymbol{q}_i, \boldsymbol{s}_i) = {^{\mathcal{B}_{i-1}}\boldsymbol{T}_{\mathcal{J}_i}}\left(\boldsymbol{q}_{\mathcal{J}_i}\right) {^{\mathcal{J}_i}\boldsymbol{T}_{\mathcal{B}_i}}\left(\boldsymbol{q}_{\mathcal{B}_i}, \boldsymbol{s}_i\right). \quad (4)$$

It is worth observing that the computation of the kinematics and dynamics requires only the homogeneous transformation from one body to its predecessor. Indeed, the only effect of the joints, which can be considered mass-less bodies, is to impose motion constraints between the bodies of the chain. In the following, for the sake of simplicity, we write $^{i-1}\boldsymbol{T}_i = {^{\mathcal{B}_{i-1}}\boldsymbol{T}_{\mathcal{B}_i}}$ and omit the superscript ^{0} for quantities expressed in the base frame.

Using (4), one can compute by concatenation the homogeneous transformation $\boldsymbol{T}_i$ from each point of $\mathcal{B}_i$ to the base

[2] With abuse of terminology, the terms *particle* and *point* are used as synonyms of *infinitesimal volume region*.

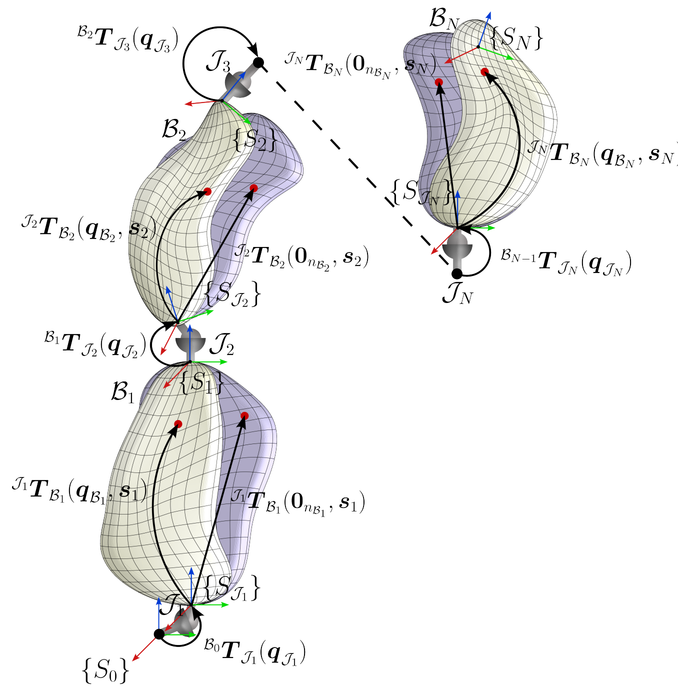

Figure 2: Sketch of a generic mechanical system, conceptualized as a sequence of bodies $\mathcal{B}_i$ and joints $\mathcal{J}_i$. Two types of reference frames are introduced to describe the motion: one for each point of $\mathcal{B}_i$ and another for $\mathcal{J}_i$, denoted as $\{S_{\mathcal{B}_i}(\boldsymbol{s}_i)\}$ and $\{S_{\mathcal{J}_i}\}$, respectively. The transformation matrix $^{\mathcal{B}_{i-1}}\boldsymbol{T}_{\mathcal{J}_i}\left(\boldsymbol{q}_{\mathcal{J}_i}\right)$ encapsulates the relative motion, due to the joint, between $\mathcal{B}_i$ and its predecessor. To account for the presence of deformable bodies, a second transformation $^{\mathcal{J}_i}\boldsymbol{T}_{\mathcal{B}_i}\left(\boldsymbol{q}_{\mathcal{B}_i}, \boldsymbol{s}_i\right)$ describes the position and orientation of each body infinitesimal volume with respect to $\mathcal{J}_i$.

$$\begin{aligned} \boldsymbol{T}_i(\boldsymbol{q}_1, \cdots, \boldsymbol{q}_i, \boldsymbol{s}_i) &= \boldsymbol{T}_1(\boldsymbol{q}_1, \boldsymbol{s}_{\mathcal{J}_2})^1\boldsymbol{T}_2(\boldsymbol{q}_2, \boldsymbol{s}_{\mathcal{J}_3}) \\ &\quad \ldots {^{i-1}\boldsymbol{T}_i}(\boldsymbol{q}_i, \boldsymbol{s}_i) \\ &= \begin{pmatrix} \boldsymbol{R}_i & \boldsymbol{t}_i \\ \boldsymbol{0}_{1\times 3} & 1 \end{pmatrix}. \end{aligned} \quad (5)$$

The above equation completely characterizes the kinematics of the system and can be differentiated with respect to time to obtain the velocity and acceleration of each particle. Note also that the only material coordinate affecting $\boldsymbol{T}_i$ is $\boldsymbol{s}_i$.

A. First- and second-order differential kinematics

We now employ (5) to compute the differential kinematics. The derivation process parallels the steps undertaken for a rigid system. However, in this context, additional terms emerge due to deformations within the body.

Denote with $^i\boldsymbol{p}_i(\boldsymbol{q}_i, \boldsymbol{s}_i) \in \mathbb{R}^3$ the position of a point of $\mathcal{B}_i$ relative to $\mathcal{B}_{i-1}$, expressed in the body frame $\{S_i\}$. Remarkably, $^i\boldsymbol{p}_i(\boldsymbol{q}_i, \boldsymbol{s}_i)$ can be computed from (4) as

$$\begin{aligned} ^i\boldsymbol{p}_i(\boldsymbol{q}_i, \boldsymbol{s}_i) = {^{i-1}\boldsymbol{R}_i^T}(\boldsymbol{q}_i, \boldsymbol{s}_{\mathcal{J}_{i+1}}) \big(& {^{i-1}\boldsymbol{t}_i}(\boldsymbol{q}_i, \boldsymbol{s}_i) \\ & - {^{i-1}\boldsymbol{t}_i}(\boldsymbol{q}_i, \boldsymbol{s}_{\mathcal{J}_{i+1}}) \big), \end{aligned}$$

Furthermore, let the center of mass of $\mathcal{B}_i$ the point having position in $\{S_i\}$ given by

$$^i\boldsymbol{p}_{\mathrm{CoM}_i}(\boldsymbol{q}_i) = \frac{1}{m_i} \int_{V_i} {^i\boldsymbol{p}_i}(\boldsymbol{q}_i, \boldsymbol{s}_i) \rho_i(\boldsymbol{s}_i) \mathrm{d}V,$$

$$
{}^{\mathcal{B}_{i-1}}\boldsymbol{T}_{\mathcal{J}_i}\left(q_{\mathcal{J}_i}\right) = \begin{pmatrix} \cos(q_{\mathcal{J}_i}) & -\sin(q_{\mathcal{J}_i}) & 0 & 0 \\ \sin(q_{\mathcal{J}_i}) & \cos(q_{\mathcal{J}_i}) & 0 & 0 \\ 0 & 0 & 1 & 0 \\ 0 & 0 & 0 & 1 \end{pmatrix},
$$

(a) Revolute joint; $q_{\mathcal{J}_i} \in [0; 2\pi)$

$$
{}^{\mathcal{B}_{i-1}}\boldsymbol{T}_{\mathcal{J}_i}\left(q_{\mathcal{J}_i}\right) = \begin{pmatrix} 1 & 0 & 0 & q_{\mathcal{J}_i} \\ 0 & 1 & 0 & 0 \\ 0 & 0 & 1 & 0 \\ 0 & 0 & 0 & 1 \end{pmatrix},
$$

(b) Prismatic joint; $q_{\mathcal{J}_i} \in \mathbb{R}$

$$
{}^{\mathcal{B}_{i-1}}\boldsymbol{T}_{\mathcal{J}_i} = \boldsymbol{I}_4,
$$

(c) Fixed joint; $q_{\mathcal{J}_i} \in \varnothing$

$$
{}^{\mathcal{J}_i}\boldsymbol{T}_{\mathcal{B}_i}\left(q_{\mathcal{B}_i}, s_i\right) = \begin{pmatrix} \cos(\frac{s_i}{L_{0_i}}\, q_{\mathcal{B}_i}) & -\sin(\frac{s_i}{L_{0_i}}\, q_{\mathcal{B}_i}) & 0 & L_{0_i}\dfrac{\sin(\frac{s_i}{L_{0_i}}\, q_{\mathcal{B}_i})}{q_{\mathcal{B}_i}} \\ \sin(\frac{s_i}{L_{0_i}}\, q_{\mathcal{B}_i}) & \cos(\frac{s_i}{L_{0_i}}\, q_{\mathcal{B}_i}) & 0 & L_{0_i}\dfrac{1-\cos(\frac{s_i}{L_{0_i}}\, q_{\mathcal{B}_i})}{q_{\mathcal{B}_i}} \\ 0 & 0 & 1 & 0 \\ 0 & 0 & 0 & 1 \end{pmatrix},
$$

(d) Planar PCC body without elongation; $q_{\mathcal{B}_i} \in \mathbb{R}$ and $s_i \in [0, L_{0_i}]$

$$
{}^{\mathcal{J}_i}\boldsymbol{T}_{\mathcal{B}_i}\left(\boldsymbol{s}_i\right) = \begin{pmatrix} 1 & 0 & 0 & t_x(\boldsymbol{s}_i) \\ 0 & 1 & 0 & t_y(\boldsymbol{s}_i) \\ 0 & 0 & 1 & t_z(\boldsymbol{s}_i) \\ 0 & 0 & 0 & 1 \end{pmatrix},
$$

(e) Rigid body; $q_{\mathcal{B}_i} \in \varnothing$ and $\boldsymbol{s}_i \in V_i$

Figure 3: Examples of homogeneous transformations from joints to predecessor bodies (a)–(c) and from bodies to joints (d)–(e).

where $m_i = \int_{V_i} \rho_i(\boldsymbol{s}_i)\mathrm{d}V$ is the body mass and $\rho_i(\boldsymbol{s}_i)$ its mass density. Since ${}^i\boldsymbol{p}_i$ and ${}^i\boldsymbol{p}_{\mathrm{CoM}_i}$ are elements of $\mathbb{R}^3$, there exists always a unique vector ${}^i\boldsymbol{r}_i \in \mathbb{R}^3$ such that the following holds

$$
{}^i\boldsymbol{p}_i = {}^i\boldsymbol{r}_i + {}^i\boldsymbol{p}_{\mathrm{CoM}_i}, \tag{6}
$$

where ${}^i\boldsymbol{r}_i$ satisfies the notable property

$$
\int_{V_i} {}^i\boldsymbol{r}_i \rho_i \mathrm{d}V = \int_{V_i} {}^i\boldsymbol{p}_i \rho_i \mathrm{d}V - {}^i\boldsymbol{p}_{\mathrm{CoM}_i} \int_{V_i} \rho_i \mathrm{d}V = \boldsymbol{0}_{3\times 1}. \tag{7}
$$

The above identity can be exploited to simplify the EoM, as usually done for rigid-bodied systems, and it allows to decompose the motion of each body in terms of its rigid and deformable parts.

Remark 2. *In the flexible link case, ${}^i\boldsymbol{r}_i$ is typically approximated following a modal-Ritz reduction approach, i.e.,*

$$
{}^i\boldsymbol{r}_i(\boldsymbol{q}_{\mathcal{B}_i}, \boldsymbol{s}_i) = \boldsymbol{\Phi}_{\boldsymbol{r}_i}(\boldsymbol{s}_i)\boldsymbol{q}_{\mathcal{B}_i}.
$$

In this this work, we never consider such hypothesis. In fact, we assume a generic and unknown functional dependence of ${}^i\boldsymbol{r}_i$ on $\boldsymbol{q}_{\mathcal{B}_i}$ and $\boldsymbol{s}_i$.

In view of (5) and (6), we can express ${}^i\boldsymbol{p}_i$ and ${}^i\boldsymbol{p}_{\mathrm{CoM}_i}$ in the base frame as

$$
\boldsymbol{p}_i = \boldsymbol{p}_{\mathrm{CoM}_i} + \boldsymbol{R}_i {}^i\boldsymbol{r}_i,
$$

and

$$
\boldsymbol{p}_{\mathrm{CoM}_i} = \boldsymbol{t}_i + \boldsymbol{R}_i {}^i\boldsymbol{p}_{\mathrm{CoM}_i}.
$$

Time differentiating the above expressions yields the linear velocity of the center of mass and that of each body, i.e.,

$$
\boldsymbol{v}_{\mathrm{CoM}_i} = \dot{\boldsymbol{p}}_{\mathrm{CoM}_i} = \boldsymbol{v}_i + \boldsymbol{\omega}_i \times \boldsymbol{R}_i {}^i\boldsymbol{p}_{\mathrm{CoM}_i} + \boldsymbol{R}_i {}^i\dot{\boldsymbol{p}}_{\mathrm{CoM}_i}, \tag{8}
$$

$$
\dot{\boldsymbol{p}}_i = \boldsymbol{v}_{\mathrm{CoM}_i} + \boldsymbol{\omega}_i \times \boldsymbol{R}_i {}^i\boldsymbol{r}_i + \boldsymbol{R}_i {}^i\dot{\boldsymbol{r}}_i, \tag{9}
$$

where $\boldsymbol{v}_i = \dot{\boldsymbol{t}}_i$ and $\boldsymbol{\omega}_i = \left(\dot{\boldsymbol{R}}_i \boldsymbol{R}_i^T\right)^\vee$ are the linear and angular velocity of $\{S_i\}$ in $\{S_0\}$, respectively. Observing that $\boldsymbol{t}_i = \boldsymbol{t}_{i-1} + \boldsymbol{R}_{i-1} {}^{i-1}\boldsymbol{t}_i$, it is possible to verify that $\boldsymbol{v}_i$ and $\boldsymbol{\omega}_i$ admit the following recursive expressions

$$
\boldsymbol{v}_i = \boldsymbol{v}_{i-1} + \boldsymbol{\omega}_{i-1} \times \boldsymbol{R}_{i-1} {}^{i-1}\boldsymbol{t}_i + \boldsymbol{R}_{i-1} {}^{i-1}\boldsymbol{v}_{i-1,i}, \tag{10}
$$

$$
\boldsymbol{\omega}_i = \boldsymbol{\omega}_{i-1} + \boldsymbol{R}_{i-1} {}^{i-1}\boldsymbol{\omega}_{i-1,i}, \tag{11}
$$

being ${}^{i-1}\boldsymbol{v}_{i-1,i} = {}^{i-1}\dot{\boldsymbol{t}}_i$ and ${}^{i-1}\boldsymbol{\omega}_{i-1,i} = \left({}^{i-1}\dot{\boldsymbol{R}}_i {}^{i-1}\boldsymbol{R}_i^T\right)^\vee$ the relative linear and angular velocity of $\{S_i\}$ as seen from $\{S_{i-1}\}$. Note that the above formulas also appear in procedures that compute the FD and ID for rigid systems [16]. However, the right-hand side of (8) and (9) contains the additional terms $\boldsymbol{R}_i {}^i\dot{\boldsymbol{p}}_{\mathrm{CoM}_i}$ and $\boldsymbol{R}_i {}^i\dot{\boldsymbol{r}}_i$, which account for the relative motions of the center of mass and of the body particles with respect to the reference configuration.

For the following derivations, it is also convenient to define the velocity vectors in the body frame $\{S_i\}$, namely

$$
{}^i\boldsymbol{v}_i = \boldsymbol{R}_i^T \boldsymbol{v}_i,\ {}^i\boldsymbol{\omega}_i = \boldsymbol{R}_i^T \boldsymbol{\omega}_i,\ {}^i\boldsymbol{v}_{\mathrm{CoM}_i} = \boldsymbol{R}_i^T \boldsymbol{v}_{\mathrm{CoM}_i}.
$$

Making use of (10) and (11), one obtains the following recursive expressions

$$
{}^i\boldsymbol{v}_i = {}^{i-1}\boldsymbol{R}_i^T({}^{i-1}\boldsymbol{v}_{i-1} + {}^{i-1}\boldsymbol{\omega}_{i-1} \times {}^{i-1}\boldsymbol{t}_i + {}^{i-1}\boldsymbol{v}_{i-1,i}), \tag{12}
$$

$$
{}^i\boldsymbol{\omega}_i = {}^{i-1}\boldsymbol{R}_i^T({}^{i-1}\boldsymbol{\omega}_{i-1} + {}^{i-1}\boldsymbol{\omega}_{i-1,i}), \tag{13}
$$

$$
{}^i\boldsymbol{v}_{\mathrm{CoM}_i} = {}^i\boldsymbol{v}_i + {}^i\boldsymbol{\omega}_i \times {}^i\boldsymbol{p}_{\mathrm{CoM}_i} + {}^i\dot{\boldsymbol{p}}_{\mathrm{CoM}_i}, \tag{14}
$$

with ${}^0\boldsymbol{v}_0 = \boldsymbol{0}_{3\times 1}\ [\mathrm{m\,s^{-1}}]$ and ${}^0\boldsymbol{\omega}_0 = \boldsymbol{0}_{3\times 1}\ [\mathrm{rad\,s^{-1}}]$.

Since the formulation of the dynamics requires the accelerations, we time differentiate also (8), (10) and (11), obtaining

$$
\begin{aligned}
\boldsymbol{a}_{\mathrm{CoM}_i} = \frac{\mathrm{d}\boldsymbol{v}_{\mathrm{CoM}_i}}{\mathrm{d}t} &= \boldsymbol{a}_i + \dot{\boldsymbol{\omega}}_i \times \boldsymbol{R}_i {}^i\boldsymbol{p}_{\mathrm{CoM}_i} + \boldsymbol{\omega}_i \\
&\quad \times \left(\boldsymbol{\omega}_i \times \boldsymbol{R}_i {}^i\boldsymbol{p}_{\mathrm{CoM}_i} + \boldsymbol{R}_i {}^i\dot{\boldsymbol{p}}_{\mathrm{CoM}_i}\right) \\
&\quad + \boldsymbol{\omega}_i \times \boldsymbol{R}_i {}^i\dot{\boldsymbol{p}}_{\mathrm{CoM}_i} + \boldsymbol{R}_i {}^i\ddot{\boldsymbol{p}}_{\mathrm{CoM}_i},
\end{aligned}
$$

$$
\begin{aligned}
\boldsymbol{a}_i = \frac{\mathrm{d}\boldsymbol{v}_i}{\mathrm{d}t} &= \boldsymbol{a}_{i-1} + \dot{\boldsymbol{\omega}}_{i-1} \times \boldsymbol{R}_{i-1} {}^{i-1}\boldsymbol{t}_i + \boldsymbol{\omega}_{i-1} \\
&\quad \times \left(\boldsymbol{\omega}_{i-1} \times \boldsymbol{R}_{i-1} {}^{i-1}\boldsymbol{t}_i + \boldsymbol{R}_{i-1} {}^{i-1}\boldsymbol{v}_{i-1,i}\right) \\
&\quad + \boldsymbol{\omega}_{i-1} \times \boldsymbol{R}_{i-1} {}^{i-1}\boldsymbol{v}_{i-1,i} + \boldsymbol{R}_{i-1} {}^{i-1}\dot{\boldsymbol{v}}_{i-1,i},
\end{aligned}
$$

and

$$
\begin{aligned}
\dot{\boldsymbol{\omega}}_i = \frac{\mathrm{d}\boldsymbol{\omega}_i}{\mathrm{d}t} &= \dot{\boldsymbol{\omega}}_{i-1} + \boldsymbol{\omega}_{i-1} \times \boldsymbol{R}_{i-1} {}^{i-1}\boldsymbol{\omega}_{i-1,i} \\
&\quad + \boldsymbol{R}_{i-1} {}^{i-1}\dot{\boldsymbol{\omega}}_{i-1,i}.
\end{aligned}
$$

From (9) and the above equations, it follows immediately that

$$
\begin{aligned}
\ddot{\boldsymbol{p}}_i &= \boldsymbol{a}_{\mathrm{CoM}_i} + \dot{\boldsymbol{\omega}}_i \times \boldsymbol{R}_i {}^i\boldsymbol{r}_i + \boldsymbol{\omega}_i \times (\boldsymbol{\omega}_i \times \boldsymbol{R}_i {}^i\boldsymbol{r}_i) \\
&\quad + 2\boldsymbol{\omega}_i \times \boldsymbol{R}_i {}^i\dot{\boldsymbol{r}}_i + \boldsymbol{R}_i {}^i\ddot{\boldsymbol{r}}_i.
\end{aligned} \tag{15}
$$

Rotating the above vectors again in the body frame, i.e.,

$$^{i}\boldsymbol{a}_i = \boldsymbol{R}_i^T \boldsymbol{v}_i,\ ^{i}\dot{\boldsymbol{\omega}}_i = \boldsymbol{R}_i^T \boldsymbol{\omega}_i,\ ^{i}\boldsymbol{a}_{\mathrm{CoM}_i} = \boldsymbol{R}_i^T \boldsymbol{v}_{\mathrm{CoM}_i},$$

some computations lead to

$$\begin{aligned} ^{i}\boldsymbol{a}_i = {}^{i-1}\boldsymbol{R}_i^T \big[&{}^{i-1}\boldsymbol{a}_{i-1} + {}^{i-1}\dot{\boldsymbol{\omega}}_{i-1} \times {}^{i-1}\boldsymbol{t}_i \\ &+ {}^{i-1}\boldsymbol{\omega}_{i-1} \times \left({}^{i-1}\boldsymbol{\omega}_{i-1} \times {}^{i-1}\boldsymbol{t}_i + {}^{i-1}\boldsymbol{v}_{i-1,i}\right) \\ &+ {}^{i-1}\boldsymbol{\omega}_{i-1} \times {}^{i-1}\boldsymbol{v}_{i-1,i} + {}^{i-1}\dot{\boldsymbol{v}}_{i-1,i}\big], \end{aligned} \tag{16}$$

$$\begin{aligned} ^{i}\dot{\boldsymbol{\omega}}_i = {}^{i-1}\boldsymbol{R}_i^T \big(&{}^{i-1}\dot{\boldsymbol{\omega}}_{i-1} + {}^{i-1}\boldsymbol{\omega}_{i-1} \times {}^{i-1}\boldsymbol{\omega}_{i-1,i} \\ &+ {}^{i-1}\dot{\boldsymbol{\omega}}_{i-1,i}\big), \end{aligned} \tag{17}$$

$$\begin{aligned} ^{i}\boldsymbol{a}_{\mathrm{CoM}_i} = {}&{}^{i}\boldsymbol{a}_i + {}^{i}\dot{\boldsymbol{\omega}}_i \times {}^{i}\boldsymbol{p}_{\mathrm{CoM}_i} \\ &+ {}^{i}\boldsymbol{\omega}_i \times \left({}^{i}\boldsymbol{\omega}_i \times {}^{i}\boldsymbol{p}_{\mathrm{CoM}_i} + {}^{i}\dot{\boldsymbol{p}}_{\mathrm{CoM}_i}\right) \\ &+ {}^{i}\boldsymbol{\omega}_i \times {}^{i}\dot{\boldsymbol{p}}_{\mathrm{CoM}_i} + {}^{i}\ddot{\boldsymbol{p}}_{\mathrm{CoM}_i}, \end{aligned} \tag{18}$$

and

$$\begin{aligned} ^{i}\ddot{\boldsymbol{p}}_i = {}&{}^{i}\boldsymbol{a}_{\mathrm{CoM}_i} + {}^{i}\dot{\boldsymbol{\omega}}_i \times {}^{i}\boldsymbol{r}_i + {}^{i}\boldsymbol{\omega}_i \times ({}^{i}\boldsymbol{\omega}_i \times {}^{i}\boldsymbol{r}_i) \\ &+ 2\,{}^{i}\boldsymbol{\omega}_i \times {}^{i}\dot{\boldsymbol{r}}_i + \boldsymbol{R}_i {}^{i}\ddot{\boldsymbol{r}}_i. \end{aligned} \tag{19}$$

The following result is an immediate consequence of the above equations.

Lemma 1. *Given $\boldsymbol{q}, \dot{\boldsymbol{q}}$ and $\ddot{\boldsymbol{q}}$, the first- and second-order differential kinematics expressed in the body frame, i.e., ${}^{i}\boldsymbol{v}_i, {}^{i}\boldsymbol{\omega}_i, {}^{i}\boldsymbol{v}_{\mathrm{CoM}_i}, {}^{i}\boldsymbol{a}_i, {}^{i}\dot{\boldsymbol{\omega}}_i$ and $\boldsymbol{a}_{\mathrm{CoM}_i}$, can be computed recursively forward in space from $\mathcal{B}_1$ to $\mathcal{B}_N$ with ${}^{0}\boldsymbol{v}_0 = \boldsymbol{0}_{3\times1}$ $[\mathrm{m\,s^{-1}}]$, ${}^{0}\boldsymbol{\omega}_0 = \boldsymbol{0}_{3\times1}$ $[\mathrm{rad\,s^{-1}}]$, ${}^{0}\boldsymbol{a}_0 = \boldsymbol{0}_{3\times1}$ $[\mathrm{m\,s^{-2}}]$ and ${}^{0}\dot{\boldsymbol{\omega}}_0 = \boldsymbol{0}_{3\times1}$ $[\mathrm{rad\,s^{-2}}]$. In addition, the computational complexity for such evaluation is $O(N)$.*

Proof. The result follows by observing the recursive structure of (12)–(14) and (16)–(18) and that their right-hand sides depend only on $\boldsymbol{q}_j$, $\dot{\boldsymbol{q}}_j$ and $\ddot{\boldsymbol{q}}_j; j \in \{1, \cdots, i\}$. □

Furthermore, it is worth anticipating that, in analogy with the rigid body case, the computation of the differential kinematics will constitute the first step of the ID procedure.

III. Kane Equations

In this section, we briefly derive the Kane equations for a modular mechanical system, as introduced in Sec. II. The derivation entails a two-step procedure. In particular, starting from the weak formulation of the dynamics, the equations are projected in the configuration space defined by $\boldsymbol{q}$.

According to the weak form of the EoM [51], for every body $\mathcal{B}_i$ of the system, one has

$$\int_{V_i} \delta\boldsymbol{p}_i^T \left(\boldsymbol{f}_{\mathrm{int}_i} + \boldsymbol{f}_{\mathrm{ext}_i} - \frac{\mathrm{d}\left(\dot{\boldsymbol{p}}_i \rho_i\right)}{\mathrm{d}t}\right) \mathrm{d}V = 0. \tag{20}$$

Here, $\boldsymbol{f}_{\mathrm{int}_i}$ is the vector modeling internal forces per unit volume, such as the mechanical stress and actuation forces (when the system is internally actuated). The vector $\boldsymbol{f}_{\mathrm{ext}_i}$ represents the resultant external force per unit volume, including for example gravity. Furthermore, $\frac{\mathrm{d}(\dot{\boldsymbol{p}}_i \rho_i)}{\mathrm{d}t}$ is the time derivative of the particle linear momentum per unit volume. According to the Kane method, in the computations, it suffices to consider among $\boldsymbol{f}_{\mathrm{int}_i}$ and $\boldsymbol{f}_{\mathrm{ext}_i}$ only the forces that perform work on the body particles, i.e., the forces for which $\int_{V_i} \delta\boldsymbol{p}_i^T \boldsymbol{f}_{\mathrm{int}_i} \mathrm{d}V \neq 0$ and $\int_{V_i} \delta\boldsymbol{p}_i^T \boldsymbol{f}_{\mathrm{ext}_i} \mathrm{d}V \neq 0$. For example, the reaction forces between two consecutive bodies are non-working. As a result, they can be neglected in the balance equation.

Recalling that the time dependence of $\boldsymbol{p}_i$ is implicit and solely through $\boldsymbol{q}$, it follows that $\delta\boldsymbol{p}_i = \left(\nabla_{\boldsymbol{q}} \boldsymbol{p}_i\right)^T \delta\boldsymbol{q}$. Substituting this into the above equation and rearranging the terms yields

$$\int_{V_i} \delta\boldsymbol{q}^T \nabla_{\boldsymbol{q}} \boldsymbol{p}_i \left(\mathrm{d}\boldsymbol{f}_i - \frac{\mathrm{d}\left(\dot{\boldsymbol{p}}_i \rho_i\right)}{\mathrm{d}t}\right) = 0,$$

where we have defined for compactness the net force $\mathrm{d}\boldsymbol{f}_i = \left(\boldsymbol{f}_{\mathrm{int}_i} + \boldsymbol{f}_{\mathrm{ext}_i}\right)\mathrm{d}V$. Since the system is holonomic, each generalized coordinate can experience a virtual displacement independently of the others, which implies

$$\int_{V_i} \nabla_{\boldsymbol{q}} \boldsymbol{p}_i \left(\mathrm{d}\boldsymbol{f}_i - \frac{\mathrm{d}\left(\dot{\boldsymbol{p}}_i \rho_i\right)}{\mathrm{d}t}\mathrm{d}V\right) = \boldsymbol{0}_n.$$

Summing the contributions for each body gives the reduced-order EoM

$$\sum_{i=1}^{N} \int_{V_i} \nabla_{\boldsymbol{q}} \boldsymbol{p}_i \left(\mathrm{d}\boldsymbol{f}_i - \frac{\mathrm{d}\left(\dot{\boldsymbol{p}}_i \rho_i\right)}{\mathrm{d}t}\mathrm{d}V\right) = \boldsymbol{0}_n,$$

and the Kane equations for the system

$$\boldsymbol{Q} = \sum_{i=1}^{N} \int_{V_i} \nabla_{\dot{\boldsymbol{q}}} \dot{\boldsymbol{p}}_i \mathrm{d}\boldsymbol{f}_i, \tag{21}$$

$$\boldsymbol{Q}^* = -\sum_{i=1}^{N} \int_{V_i} \nabla_{\dot{\boldsymbol{q}}} \dot{\boldsymbol{p}}_i \frac{\mathrm{d}\left(\dot{\boldsymbol{p}}_i \rho_i\right)}{\mathrm{d}t}\mathrm{d}V, \tag{22}$$

$$\boldsymbol{Q} + \boldsymbol{Q}^* = \boldsymbol{0}_n, \tag{23}$$

where the identity $\nabla_{\boldsymbol{q}} \boldsymbol{p}_i = \nabla_{\dot{\boldsymbol{q}}} \dot{\boldsymbol{p}}_i$ has been used. The terms $\boldsymbol{Q}$ and $\boldsymbol{Q}^*$ are called the generalized active and inertia force, respectively. In the following, for the sake of simplicity, we restrict the analysis to systems for which the variation of the mass density is negligible, i.e., $\dot{\rho}_i = 0$, $i \in \{1, \cdots, N\}$. This way, we can simplify the second term in the integrand of (22) as

$$\frac{\mathrm{d}\left(\dot{\boldsymbol{p}}_i \rho_i\right)}{\mathrm{d}t}\mathrm{d}V = \ddot{\boldsymbol{p}}_i \rho_i \mathrm{d}V = \ddot{\boldsymbol{p}}_i \mathrm{d}m_i, \tag{24}$$

where we defined the infinitesimal mass $\mathrm{d}m_i = \rho_i \mathrm{d}V$. From (7) and the Reynolds transport theorem, this also implies

$$\int_{V_i} {}^{i}\dot{\boldsymbol{r}}_i \rho_i \mathrm{d}V = \frac{\mathrm{d}}{\mathrm{d}t}\left(\int_{V_i} {}^{i}\boldsymbol{r}_i \rho_i \mathrm{d}V\right) = \boldsymbol{0}_{3\times1}, \tag{25}$$

and

$$\int_{V_i} {}^{i}\ddot{\boldsymbol{r}}_i \rho_i \mathrm{d}V = \frac{\mathrm{d}}{\mathrm{d}t}\left(\int_{V_i} {}^{i}\dot{\boldsymbol{r}}_i \rho_i \mathrm{d}V\right) = \boldsymbol{0}_{3\times1}. \tag{26}$$

It is worth underlying that the above hypothesis can be relaxed at the price of longer expressions in the recursive formulation.

Proposition 2. *Equations* (21)–(24) *are equivalent to* (1)*, i.e.,*

$$-\boldsymbol{Q}^*(\boldsymbol{q}, \dot{\boldsymbol{q}}, \ddot{\boldsymbol{q}}) = \boldsymbol{M}(\boldsymbol{q})\ddot{\boldsymbol{q}} + \boldsymbol{n}(\boldsymbol{q}, \dot{\boldsymbol{q}}). \tag{27}$$

Proof. See Appendix A □

In the following, we establish a recursive expression of (21)-(23), which allows an efficient computation of $\boldsymbol{Q}$ and $\boldsymbol{Q}^*$. For the sake of derivation, it proves advantageous to expand $\boldsymbol{Q}$ and $\boldsymbol{Q}^*$ into their components of the single bodies. This involves considering the EoM (21)–(23) in the equivalent form

$$\boldsymbol{Q}_j = \sum_{i=1}^{N} \int_{V_i} \nabla_{\dot{\boldsymbol{q}}_j} \dot{\boldsymbol{p}}_i \mathrm{d}\boldsymbol{f}_i, \tag{28}$$

$$\boldsymbol{Q}_j^* = -\sum_{i=1}^{N} \int_{V_i} \nabla_{\dot{\boldsymbol{q}}_j} \dot{\boldsymbol{p}}_i \ddot{\boldsymbol{p}}_i \mathrm{d}m_i, \tag{29}$$

$$\boldsymbol{Q}_j + \boldsymbol{Q}_j^* = \boldsymbol{0}_{n_j}, \tag{30}$$

with $j \in \{1, \cdots, N\}$, where we expanded $\boldsymbol{Q}$ and $\boldsymbol{Q}^*$ into their components associated to each body $\mathcal{B}_j$.

IV. Recursive Formulation of the Equations of Motion

This section presents the main result of the paper, i.e., a recursive formulation of (28)–(30), which yields a simple and general procedure for the solution of the IDP. We provide a pseudo-code for implementing the algorithm, encompassing all necessary terms. Remarkably, the treatment remains independent on the assumption that $\dot{\rho}_i = 0$.

To this end, rewrite the left-hand side of (30) explicitly for $\boldsymbol{q}_j$ as

$$\boldsymbol{Q}_j + \boldsymbol{Q}_j^* = \sum_{i=1}^{N} \int_{V_i} \nabla_{\dot{\boldsymbol{q}}_j} \dot{\boldsymbol{p}}_i \left(\mathrm{d}\boldsymbol{f}_i - \ddot{\boldsymbol{p}}_i \mathrm{d}m_i\right).$$

Note that, for $i < j$, $\nabla_{\dot{\boldsymbol{q}}_j} \dot{\boldsymbol{p}}_i = \boldsymbol{0}_{n_j \times 3}$ because $\boldsymbol{p}_i$ depends only on $\boldsymbol{q}_1, \ldots, \boldsymbol{q}_{i-1}$ and $\boldsymbol{q}_i$. Consequently, the lower bound of the summation can be replaced with the index associated with $\mathcal{B}_j$, leading to a more concise form

$$\boldsymbol{Q}_j + \boldsymbol{Q}_j^* = \sum_{i=j}^{N} \int_{V_i} \nabla_{\dot{\boldsymbol{q}}_j} \dot{\boldsymbol{p}}_i \left(\mathrm{d}\boldsymbol{f}_i - \ddot{\boldsymbol{p}}_i \mathrm{d}m_i\right).$$

By leveraging (9), the previous equation can be rewritten as

$$\begin{aligned}\boldsymbol{Q}_j + \boldsymbol{Q}_j^* = &\sum_{i=j}^{N} \nabla_{\dot{\boldsymbol{q}}_j} \boldsymbol{v}_{\mathrm{CoM}_i} \int_{V_i} \mathrm{d}\boldsymbol{f}_i - \ddot{\boldsymbol{p}}_i \mathrm{d}m_i \\ &+ \nabla_{\dot{\boldsymbol{q}}_j} \boldsymbol{\omega}_i \int_{V_i} \left(\boldsymbol{R}_i {}^i\boldsymbol{r}_i\right) \times \left(\mathrm{d}\boldsymbol{f}_i - \ddot{\boldsymbol{p}}_i \mathrm{d}m_i\right) \\ &+ \int_{V_i} \nabla_{\dot{\boldsymbol{q}}_j} {}^i\dot{\boldsymbol{r}}_i \boldsymbol{R}_i^T \left(\mathrm{d}\boldsymbol{f}_i - \ddot{\boldsymbol{p}}_i \mathrm{d}m_i\right).\end{aligned}$$

Given that ${}^i\boldsymbol{r}_i$ depends solely on the configuration variables of the corresponding body $\mathcal{B}_i$, it holds $\nabla_{\dot{\boldsymbol{q}}_j} {}^i\dot{\boldsymbol{r}}_i = \boldsymbol{0}_{n_j \times 3};\ i \neq j$, which simplifies the above expression to

$$\begin{aligned}\boldsymbol{Q}_j + \boldsymbol{Q}_j^* = &\int_{V_j} \nabla_{\dot{\boldsymbol{q}}_j} {}^j\dot{\boldsymbol{r}}_j \boldsymbol{R}_j^T \left(\mathrm{d}\boldsymbol{f}_j - \ddot{\boldsymbol{p}}_j \mathrm{d}m_j\right) \\ &+ \sum_{i=j}^{N} \nabla_{\dot{\boldsymbol{q}}_j} \boldsymbol{v}_{\mathrm{CoM}_i} \int_{V_i} \mathrm{d}\boldsymbol{f}_i - \ddot{\boldsymbol{p}}_i \mathrm{d}m_i \\ &+ \nabla_{\dot{\boldsymbol{q}}_j} \boldsymbol{\omega}_i \int_{V_i} \mathrm{d}\boldsymbol{\tau}_i - \left(\boldsymbol{R}_i {}^i\boldsymbol{r}_i\right) \times \ddot{\boldsymbol{p}}_i \mathrm{d}m_i,\end{aligned} \tag{31}$$

being $\mathrm{d}\boldsymbol{\tau}_i = \left(\boldsymbol{R}_i {}^i\boldsymbol{r}_i\right) \times \mathrm{d}\boldsymbol{f}_i$ the net torque acting on each infinitesimal volume. It should be noted that the right-hand side of the above equation contains three terms. The first models effects local to the body. On the other hand, the other two terms account for the balance of forces and momenta with respect to the center of mass. Furthermore, the summation considers the forces exchanged between $\mathcal{B}_j$ and the other bodies in the chain.

By exploiting the invariance of the scalar product for rotations, it is possible to express (31) in the body frame $\{S_i\}$ as

$$\begin{aligned}\boldsymbol{Q}_j + \boldsymbol{Q}_j^* = &\int_{V_j} \nabla_{\dot{\boldsymbol{q}}_j} {}^j\dot{\boldsymbol{r}}_j \left(\mathrm{d}^j\boldsymbol{f}_j - {}^j\ddot{\boldsymbol{p}}_j \mathrm{d}m_j\right) \\ &+ \sum_{i=j}^{N} \nabla_{\dot{\boldsymbol{q}}_j} {}^i\boldsymbol{v}_{\mathrm{CoM}_i} \int_{V_i} \mathrm{d}^i\boldsymbol{f}_i - {}^i\ddot{\boldsymbol{p}}_i \mathrm{d}m_i \\ &+ \nabla_{\dot{\boldsymbol{q}}_j} {}^i\boldsymbol{\omega}_i \int_{V_i} \mathrm{d}^i\boldsymbol{\tau}_i - {}^i\boldsymbol{r}_i \times {}^i\ddot{\boldsymbol{p}}_i \mathrm{d}m_i,\end{aligned} \tag{32}$$

where $\mathrm{d}^i\boldsymbol{f}_i = \boldsymbol{R}_i^T \mathrm{d}\boldsymbol{f}_i$ and $\mathrm{d}^i\boldsymbol{\tau}_i = \boldsymbol{R}_i^T \mathrm{d}\boldsymbol{\tau}_i$ denote the force and torque in $\{S_i\}$, respectively. For the sake of readability, we introduce the following definitions

$${}^i\boldsymbol{\mathcal{F}}_i = \int_{V_i} \mathrm{d}^i\boldsymbol{f}_i,\ {}^i\boldsymbol{\mathcal{F}}_i^* = -\int_{V_i} {}^i\ddot{\boldsymbol{p}}_i \mathrm{d}m_i,\ {}^i\boldsymbol{\mathcal{T}}_i = \int_{V_i} \mathrm{d}^i\boldsymbol{\tau}_i, \tag{33}$$

and

$${}^i\boldsymbol{\mathcal{T}}_i^* = -\int_{V_i} {}^i\boldsymbol{r}_i \times {}^i\ddot{\boldsymbol{p}}_i \mathrm{d}m_i. \tag{34}$$

Henceforth, the terms active force and torque of $\mathcal{B}_i$ denote ${}^i\boldsymbol{\mathcal{F}}_i$ and ${}^i\boldsymbol{\mathcal{T}}_i$, respectively. Similarly, ${}^i\boldsymbol{\mathcal{F}}_i^*$ and ${}^i\boldsymbol{\mathcal{T}}_i^*$ represent its inertial force and torque. Note that the dimension of all the above vectors is equal to three, independently of the number of generalized coordinates of the body. Substituting (33) into (32) leads to

$$\begin{aligned}\boldsymbol{Q}_j + \boldsymbol{Q}_j^* = &\int_{V_j} \nabla_{\dot{\boldsymbol{q}}_j} {}^j\dot{\boldsymbol{r}}_j \left({}^j\boldsymbol{\mathcal{F}}_j + {}^j\boldsymbol{\mathcal{F}}_j^*\right) \\ &+ \sum_{i=j}^{N} \nabla_{\dot{\boldsymbol{q}}_j} {}^i\boldsymbol{v}_{\mathrm{CoM}_i} \left({}^i\boldsymbol{\mathcal{F}}_i + {}^i\boldsymbol{\mathcal{F}}_i^*\right) \\ &+ \nabla_{\dot{\boldsymbol{q}}_j} {}^i\boldsymbol{\omega}_i \left({}^i\boldsymbol{\mathcal{T}}_i + {}^i\boldsymbol{\mathcal{T}}_i^*\right).\end{aligned} \tag{35}$$

The previous expression can be further simplified recalling (14), which implies that, for $i = j$,

$$\begin{aligned}\nabla_{\dot{\boldsymbol{q}}_j} {}^i\boldsymbol{v}_{\mathrm{CoM}_i} = &\nabla_{\dot{\boldsymbol{q}}_j} {}^i\boldsymbol{v}_i + \nabla_{\dot{\boldsymbol{q}}_j} {}^i\boldsymbol{\omega}_i {}^i\widetilde{\boldsymbol{p}}_{\mathrm{CoM}_i} \\ &+ \nabla_{\dot{\boldsymbol{q}}_j} {}^i\dot{\boldsymbol{p}}_{\mathrm{CoM}_i},\end{aligned}$$

and, for $i > j$,

$$\nabla_{\dot{\boldsymbol{q}}_j} {}^i\boldsymbol{v}_{\mathrm{CoM}_i} = \nabla_{\dot{\boldsymbol{q}}_j} {}^i\boldsymbol{v}_i + \nabla_{\dot{\boldsymbol{q}}_j} {}^i\boldsymbol{\omega}_i {}^i\widetilde{\boldsymbol{p}}_{\mathrm{CoM}_i}.$$

Indeed, the position of the center of mass in the body frame, and consequently also its time derivative, depends only on the configuration variables of the body. The substitution of the above identities into (35) gives

$$\boldsymbol{Q}_j + \boldsymbol{Q}_j^* = {}^j\boldsymbol{\pi}_j + {}^j\boldsymbol{\pi}_j^* + \boldsymbol{\mathcal{M}}_j\left({}^i\boldsymbol{\mathcal{F}}_i, {}^i\boldsymbol{\mathcal{F}}_i^*, {}^i\boldsymbol{\mathcal{T}}_i, {}^i\boldsymbol{\mathcal{T}}_i^*\right), \tag{36}$$

with $i \in \{j, \cdots, N\}$,

$$\begin{aligned} {}^j\boldsymbol{\pi}_j &= \int_{V_j} \nabla_{\dot{\boldsymbol{q}}_j} \left({}^j\dot{\boldsymbol{r}}_j + {}^j\dot{\boldsymbol{p}}_{\mathrm{CoM}_j} \right) \mathrm{d}^j\boldsymbol{f}_j \\ &= \int_{V_j} \nabla_{\dot{\boldsymbol{q}}_j} {}^j\dot{\boldsymbol{p}}_j \mathrm{d}^j\boldsymbol{f}_j, \end{aligned} \tag{37}$$

$$\begin{aligned} {}^j\boldsymbol{\pi}_j^* &= -\int_{V_j} \nabla_{\dot{\boldsymbol{q}}_j} \left({}^j\dot{\boldsymbol{r}}_j + {}^j\dot{\boldsymbol{p}}_{\mathrm{CoM}_j} \right) {}^j\ddot{\boldsymbol{p}}_j \mathrm{d}m_j \\ &= -\int_{V_j} \nabla_{\dot{\boldsymbol{q}}_j} {}^j\dot{\boldsymbol{p}}_j {}^j\ddot{\boldsymbol{p}}_j \mathrm{d}m_j, \end{aligned} \tag{38}$$

and

$$\begin{aligned} \boldsymbol{\mathcal{M}}_j = \sum_{i=j}^{N} & \nabla_{\dot{\boldsymbol{q}}_j} {}^i\boldsymbol{v}_i \left({}^i\boldsymbol{\mathcal{F}}_i + {}^i\boldsymbol{\mathcal{F}}_i^* \right) + \nabla_{\dot{\boldsymbol{q}}_j} {}^i\boldsymbol{\omega}_i \\ & \left({}^i\boldsymbol{\mathcal{T}}_i + {}^i\boldsymbol{\mathcal{T}}_i^* + {}^i\boldsymbol{p}_{\mathrm{CoM}_i} \times \left({}^i\boldsymbol{\mathcal{F}}_i + {}^i\boldsymbol{\mathcal{F}}_i^* \right) \right). \end{aligned} \tag{39}$$

Indeed, ${}^j\boldsymbol{\pi}_j$ and ${}^j\boldsymbol{\pi}_j^*$ contain terms that are only local to the body. In contrast, $\boldsymbol{\mathcal{M}}_j$ involves the forces and torques of $\mathcal{B}_j$ and all subsequent bodies. Consequently, only $\boldsymbol{\mathcal{M}}_j$ necessitates a recursive expression. The following theorem formalizes the main contribution of this work, namely that $\boldsymbol{\mathcal{M}}_j$ can computed recursively.

Theorem 1. *Given $\boldsymbol{q}, \dot{\boldsymbol{q}}$ and $\ddot{\boldsymbol{q}}$, the operator $\boldsymbol{\mathcal{M}}_j; j \in \{N, \cdots, 1\}$, admits the following backward recursive expression*

$$\begin{aligned} \boldsymbol{\mathcal{M}}_j = & \nabla_{\dot{\boldsymbol{q}}_j} {}^j\boldsymbol{v}_j \left({}^j\boldsymbol{F}_j + {}^j\boldsymbol{F}_j^* \right) \\ & + \nabla_{\dot{\boldsymbol{q}}_j} {}^j\boldsymbol{\omega}_j \left({}^j\boldsymbol{T}_j + {}^j\boldsymbol{T}_j^* \right), \end{aligned} \tag{40}$$

where

$$\begin{aligned} {}^j\boldsymbol{F}_j + {}^j\boldsymbol{F}_j^* = & {}^j\boldsymbol{\mathcal{F}}_j + {}^j\boldsymbol{\mathcal{F}}_j^* \\ & + {}^j\boldsymbol{R}_{j+1} \left({}^{j+1}\boldsymbol{F}_{j+1} + {}^{j+1}\boldsymbol{F}_{j+1}^* \right), \\ {}^j\boldsymbol{T}_j + {}^j\boldsymbol{T}_j^* = & {}^j\boldsymbol{\mathcal{T}}_j + {}^j\boldsymbol{\mathcal{T}}_j^* + {}^j\boldsymbol{p}_{\mathrm{CoM}_j} \times \left({}^j\boldsymbol{\mathcal{F}}_j + {}^j\boldsymbol{\mathcal{F}}_j^* \right) \\ & + {}^j\boldsymbol{R}_{j+1} \left({}^{j+1}\boldsymbol{T}_{j+1} + {}^{j+1}\boldsymbol{T}_{j+1}^* \right) \\ & + {}^j\boldsymbol{t}_{j+1} \times {}^j\boldsymbol{R}_{j+1} \left({}^{j+1}\boldsymbol{F}_{j+1} + {}^{j+1}\boldsymbol{F}_{j+1}^* \right), \end{aligned} \tag{41}$$

with ${}^{N+1}\boldsymbol{F}_{N+1} = {}^{N+1}\boldsymbol{F}_{N+1}^* = \mathbf{0}_{3\times1}$ [N] *and* ${}^{N+1}\boldsymbol{T}_{N+1} = {}^{N+1}\boldsymbol{T}_{N+1}^* = \mathbf{0}_{3\times1}$ [N m].

Proof. See Appendix B. □

In (41), the terms ${}^j\boldsymbol{F}_j$ and ${}^j\boldsymbol{T}_j$ account for the total effects of the linear and angular active forces on $\mathcal{B}_i$ due to $\mathcal{B}_i$ itself and all its successor bodies. Similarly, ${}^j\boldsymbol{F}_j^*$ and ${}^j\boldsymbol{T}_j^*$ are the corresponding inertial forces. Note that $\nabla_{\dot{\boldsymbol{q}}_j} {}^j\boldsymbol{v}_j$ and $\nabla_{\dot{\boldsymbol{q}}_j} {}^j\boldsymbol{\omega}_j$ project the system dynamics in the direction of $\boldsymbol{q}_j$ and can be computed from the kinematic model because they depend only on quantities of the body. Indeed, (12) and (13) imply

$$\nabla_{\dot{\boldsymbol{q}}_j} {}^j\boldsymbol{v}_j = \nabla_{\dot{\boldsymbol{q}}_j} {}^{j-1}\boldsymbol{v}_{j-1,j} {}^{j-1}\boldsymbol{R}_j(\boldsymbol{q}_j), \tag{42}$$

and

$$\nabla_{\dot{\boldsymbol{q}}_j} {}^j\boldsymbol{\omega}_j = \nabla_{\dot{\boldsymbol{q}}_j} {}^{j-1}\boldsymbol{\omega}_{j-1,j} {}^{j-1}\boldsymbol{R}_j(\boldsymbol{q}_j). \tag{43}$$

The derivation of the above recursive equations does not rely on the hypothesis that $\dot{\rho}_i = 0$. Indeed, the latter affects only the expression of ${}^i\boldsymbol{\mathcal{F}}_i^*$ and ${}^i\boldsymbol{\mathcal{T}}_i^*$, which depend solely on the body kinematics and mass distribution.

Remark 3. *Equations* (36)–(43) *represent a recursive form of the dynamics, parameterized by ${}^j\boldsymbol{\pi}_j, {}^j\boldsymbol{\pi}_j^*, {}^i\boldsymbol{\mathcal{F}}_i, {}^i\boldsymbol{\mathcal{F}}_i^*, {}^i\boldsymbol{\mathcal{T}}_i$ and ${}^i\boldsymbol{\mathcal{T}}_i^*$. These equations hold for any serial robotic system described by a finite number of configuration variables. Furthermore, in view of Proposition 2,* (36)–(43) *can be seen as a recursive form of the first.*

Property 1. *The operator $\boldsymbol{\mathcal{M}}_j$ is linear in all its arguments.*

Proof. The property follows from (39) since the matrix and cross products are linear operators. □

Property (1) allows isolating the contributions of the generalized active forces. This also implies that $\boldsymbol{Q}_j$ and $\boldsymbol{Q}_j^*$ can be computed by nullifying the inertial and active terms, respectively, i.e.,

$$\boldsymbol{Q}_j = {}^j\boldsymbol{\pi}_j + \boldsymbol{\mathcal{M}}_j({}^i\boldsymbol{\mathcal{F}}_i, \mathbf{0}_{3\times1}, {}^i\boldsymbol{\mathcal{T}}_i, \mathbf{0}_{3\times1}) = -\boldsymbol{Q}_j^*, \tag{44}$$

and

$$\boldsymbol{Q}_j^* = {}^j\boldsymbol{\pi}_j^* + \boldsymbol{\mathcal{M}}_j(\mathbf{0}_{3\times1}, {}^i\boldsymbol{\mathcal{F}}_i^*, \mathbf{0}_{3\times1}, {}^i\boldsymbol{\mathcal{T}}_i^*) = -\boldsymbol{Q}_j, \tag{45}$$

where the last identity in (44) and (45) arises from $\boldsymbol{Q}_j + \boldsymbol{Q}_j^* = \mathbf{0}_{n_j}$. Assuming the knowledge of ${}^i\boldsymbol{\mathcal{F}}_i^*$, ${}^i\boldsymbol{\mathcal{T}}_i^*$ and ${}^j\boldsymbol{\pi}_j^*$, the last equation offers a means of calculating $\boldsymbol{Q}_j$. Thus, the last step for solving the IDP consists of computing the inertial terms of the bodies, which we address below.

A. Evaluation of the inertial force and torque

We now evaluate the inertial terms appearing in Algorithm 1, namely ${}^i\boldsymbol{\mathcal{F}}_i^*$, ${}^i\boldsymbol{\mathcal{T}}_i^*$ and ${}^j\boldsymbol{\pi}_j^*$.

Using (15), ${}^i\boldsymbol{\mathcal{F}}_i^*$ takes the form

$${}^i\boldsymbol{\mathcal{F}}_i^* = -{}^i\boldsymbol{a}_{\mathrm{CoM}_i} m_i, \tag{46}$$

where (7) and (25)– (26) have been employed.

A similar computation for ${}^i\boldsymbol{\mathcal{T}}_i^*$ leads to

$${}^i\boldsymbol{\mathcal{T}}_i^* = -\int_{V_i} \frac{\mathrm{d}}{\mathrm{d}t} \left({}^i\boldsymbol{r}_i \times \boldsymbol{R}_i^T \frac{\mathrm{d}}{\mathrm{d}t} \left(\boldsymbol{R}_i {}^i\boldsymbol{r}_i \right) \right) \mathrm{d}m_i. \tag{47}$$

Note that the integrand of the right-hand side represents the time derivative of the particles angular momentum about the center of mass. Now, using the identity

$$\frac{\mathrm{d}}{\mathrm{d}t} \left(\boldsymbol{R}_i {}^i\boldsymbol{r}_i \right) = \boldsymbol{\omega}_i \times \boldsymbol{R}_i {}^i\boldsymbol{r}_i + \boldsymbol{R}_i {}^i\dot{\boldsymbol{r}}_i,$$

after some computations, (47) becomes

$$\begin{aligned} {}^i\boldsymbol{\mathcal{T}}_i^* = & -{}^i\boldsymbol{I}_i {}^i\dot{\boldsymbol{\omega}}_i - {}^i\boldsymbol{\omega}_i \times {}^i\boldsymbol{I}_i {}^i\boldsymbol{\omega}_i - {}^i\boldsymbol{J}_i \boldsymbol{\omega}_i - {}^i\boldsymbol{\omega}_i \\ & \times \int_{V_i} {}^i\boldsymbol{r}_i \times {}^i\dot{\boldsymbol{r}}_i \mathrm{d}m_i - \int_{V_i} {}^i\boldsymbol{r}_i \times {}^i\ddot{\boldsymbol{r}}_i \mathrm{d}m_i, \end{aligned} \tag{48}$$

where we defined the body inertia

$${}^i\boldsymbol{I}_i = \int_{V_i} {}^i\widetilde{\boldsymbol{r}}_i^T {}^i\widetilde{\boldsymbol{r}}_i \mathrm{d}m_i,$$

and its time derivative

$${}^i\boldsymbol{J}_i = \frac{\mathrm{d}^i\boldsymbol{I}_i}{\mathrm{d}t} = \int_{V_i} {}^i\dot{\widetilde{\boldsymbol{r}}}_i^T {}^i\widetilde{\boldsymbol{r}}_i + {}^i\widetilde{\boldsymbol{r}}_i^T {}^i\dot{\widetilde{\boldsymbol{r}}}_i \mathrm{d}m_i.$$

Indeed, recall that, when the body is deformable, ${}^i\boldsymbol{r}_i$ is a function of time. In addition, the first two terms on the right-hand side of (48) model the rigid motion, while the remaining terms arise because of deformability.

Now consider ${}^i\boldsymbol{\pi}_i^*$. By substituting (15) into (38) and performing some computations, one obtains

$$
\begin{aligned}
{}^i\boldsymbol{\pi}_i^* = & -\nabla_{\dot{\boldsymbol{q}}_i}\left(\int_{V_i} {}^i\boldsymbol{r}_i \times {}^i\dot{\boldsymbol{r}}_i \mathrm{d}m_i\right) {}^i\dot{\boldsymbol{\omega}}_i \\
& + \frac{1}{2}\left(\boldsymbol{I}_{n_i} \otimes \left({}^i\boldsymbol{\omega}_i^T\left({}^i\boldsymbol{\omega}_i^T \otimes \boldsymbol{I}_3\right)\right)\right) \\
& \quad \mathrm{vec}\left(\left(\nabla_{\boldsymbol{q}_i} \mathrm{vec}({}^i\boldsymbol{J}_i)\right)^T\right) \\
& - 2\left(\int_{V_i} {}^i\dot{\boldsymbol{r}}_i \times \nabla_{\dot{\boldsymbol{q}}_i} {}^i\dot{\boldsymbol{r}}_i \mathrm{d}m_i\right) {}^i\boldsymbol{\omega}_i \\
& - \int_{V_i} \nabla_{\dot{\boldsymbol{q}}_i} {}^i\dot{\boldsymbol{r}}_i {}^i\ddot{\boldsymbol{r}}_i \mathrm{d}m_i + \nabla_{\dot{\boldsymbol{q}}_i} {}^i\dot{\boldsymbol{p}}_{\mathrm{CoM}_i} {}^i\boldsymbol{\mathcal{F}}_i^*.
\end{aligned}
\tag{49}
$$

Remark 4. *All the inertial terms are functions of* $\boldsymbol{q}_i, \dot{\boldsymbol{q}}_i$ *and* $\ddot{\boldsymbol{q}}_i$ *and their functional expression can be computed offline once the kinematic model of the body and its mass density are known. When a closed-form expression for the above integrals is not available, numerical integration techniques, such as the Gaussian quadrature rule, must be used. For an in depth discussion of these methodologies see [52].*

Combining (45) with Lemma 1, Theorem 1 and the expressions for ${}^i\boldsymbol{\mathcal{F}}_i^*$, ${}^i\boldsymbol{\mathcal{T}}_i^*$ and ${}^j\boldsymbol{\pi}_j^*$, it follows that $\boldsymbol{Q}$ can be computed using Algorithm 1, denoted in the following as *Generalized ID (GID)*. In analogy with the rigid-bodied case [16], the procedure entails a forward and a backward step. In the former, $\boldsymbol{q}$ and its time derivatives are used to compute velocities and accelerations, allowing the evaluation of ${}^i\boldsymbol{\mathcal{F}}_i^*$, ${}^i\boldsymbol{\mathcal{T}}_i^*$ and ${}^j\boldsymbol{\pi}_j^*$. Then, the backward step determines the generalized inertial force by projecting the inertial terms in the configuration space. This is accomplished using (45) and its recursive formulation given by (40)–(41). The computational complexity grows linearly with the number of bodies as formalized in the following.

Corollary 1. *The computational complexity of Algorithm 1 is* $O(N)$.

Proof. From Lemma 1, (46) and (48)–(49), the cost of the forward step in Algorithm 1 is $O(N)$. Similarly, Theorem 1 implies that the computational complexity of the backward step is $O(N)$. □

It is also worth observing that, in the case where the system contains only rigid bodies, the ID for rigid robots are immediately recovered.

V. Actuation Inverse Dynamics

Usually, when solving the IDP one is interested in evaluating the contribute of the actuators only, which we denote as the *Actuation ID (AID)*, rather than of all the active forces. We address such problem in this section by separating the effect of the actuators from those of other active forces. If no other forces act on the system, then the AID and GID coincide, eliminating the need for further steps because no other forces

Algorithm 1 Generalized Inverse Dynamics: $\boldsymbol{Q}$=GID$(\boldsymbol{q}, \dot{\boldsymbol{q}}, \ddot{\boldsymbol{q}})$

Require: $\boldsymbol{q}, \dot{\boldsymbol{q}}, \ddot{\boldsymbol{q}}$
  for $i = 1 \rightarrow N_B$ **do** ▷ Forward step
    Compute ${}^i\boldsymbol{\omega}_i$, ${}^i\boldsymbol{a}_{\mathrm{CoM}_i}$ and ${}^i\dot{\boldsymbol{\omega}}_i$
    Compute ${}^i\boldsymbol{\mathcal{F}}_i^*$, ${}^i\boldsymbol{\mathcal{T}}_i^*$ and ${}^i\boldsymbol{\pi}_i^*$
  end for
  for $i = N_B \rightarrow 1$ **do** ▷ Backward step
    Compute $\boldsymbol{Q}_j$ as given in (45) by using (37)–(41)
  end for

must be considered. However, this situation seldom occurs in practice, e.g., when the robot moves in a gravitational field, and $\boldsymbol{Q}_j$ needs to be expanded into its individual components.

Being elements of vector spaces, $\mathrm{d}^i\boldsymbol{f}_i$ and $\mathrm{d}^i\boldsymbol{\tau}_i$ can be decomposed in the distinct forces and torques acting on each particle. This paper considers two additional types of generalized forces that often manifest in the robotic systems we are interested in, namely gravitational and internal interaction forces. Thus, the active force and torque take the form

$$
\mathrm{d}^i\boldsymbol{f}_i = \mathrm{d}^i\boldsymbol{f}_i^a + \mathrm{d}^i\boldsymbol{f}_i^g + \mathrm{d}^i\boldsymbol{f}_i^s, \tag{50}
$$

and

$$
\mathrm{d}^i\boldsymbol{\tau}_i = \mathrm{d}^i\boldsymbol{\tau}_i^a + \mathrm{d}^i\boldsymbol{\tau}_i^s, \tag{51}
$$

where $\mathrm{d}^i\boldsymbol{f}_i^a$, $\mathrm{d}^i\boldsymbol{f}_i^g$ and $\mathrm{d}^i\boldsymbol{f}_i^s$ denote the force due to actuation, gravity and particles interaction, respectively. The vectors $\mathrm{d}^i\boldsymbol{\tau}_i^a$ and $\mathrm{d}^i\boldsymbol{\tau}_i^s$ represent their rotational counterparts. Hence, the generalized active force can be expressed as follows

$$
\boldsymbol{Q}_j(\boldsymbol{q}, \dot{\boldsymbol{q}}, \boldsymbol{u}) = \boldsymbol{Q}_j^g(\boldsymbol{q}) + \boldsymbol{Q}_j^a(\boldsymbol{q}, \dot{\boldsymbol{q}}, \boldsymbol{u}) + \boldsymbol{Q}_j^s(\boldsymbol{q}, \dot{\boldsymbol{q}}), \tag{52}
$$

where each term on the right-hand side of the equation is obtained by replacing $\mathrm{d}\boldsymbol{f}_i$ and $\mathrm{d}\boldsymbol{\tau}_i$ with the corresponding force and torque as in (50) and (51). Note that, in view of their definition, also ${}^j\boldsymbol{\pi}_j$, ${}^i\boldsymbol{\mathcal{F}}_i$ and ${}^i\boldsymbol{\mathcal{T}}_i$ admit analogous decomposition.

Remarkably, we can immediately compute the AID without affecting the computational complexity. In particular, replacing (52) into (30) gives

$$
\boldsymbol{Q}_j^a = -\boldsymbol{Q}_j^g - \boldsymbol{Q}_j^s - \boldsymbol{Q}_j^*,
$$

or, equivalently by using (44)–(45) and the linearity of $\boldsymbol{\mathcal{M}}_j$ (Property 1),

$$
\begin{aligned}
\boldsymbol{Q}_j^a = & -{}^j\boldsymbol{\pi}_j^* - {}^j\boldsymbol{\pi}_j^s - {}^j\boldsymbol{\pi}_j^g \\
& - \boldsymbol{\mathcal{M}}_j({}^i\boldsymbol{\mathcal{F}}_i^s + {}^i\boldsymbol{\mathcal{F}}_i^g, {}^i\boldsymbol{\mathcal{F}}_i^*, {}^i\boldsymbol{\mathcal{T}}_i^s, {}^i\boldsymbol{\mathcal{T}}_i^*).
\end{aligned}
\tag{53}
$$

Note that the effect of gravity appears only as a linear force. The pseudo-code for the computation of $\boldsymbol{Q}_j^a$ is given in Algorithm 2, which is similar to that of the GID. The difference lies in accounting for the terms that correspond to external forces which differ from those generated by actuation.

We conclude this section by computing $\boldsymbol{Q}_j^g$ and $\boldsymbol{Q}_j^s$, thereby providing the complete expression of the AID.

Algorithm 2 Actuation Inverse Dynamics: $\boldsymbol{Q}^a = \mathrm{AID}(\boldsymbol{q}, \dot{\boldsymbol{q}}, \ddot{\boldsymbol{q}})$

Require: $\boldsymbol{q}, \dot{\boldsymbol{q}}, \ddot{\boldsymbol{q}}$
  for $i = 1 \to N_B$ **do** ▷ Forward step
    Compute ${}^i\boldsymbol{\omega}_i$, ${}^i\boldsymbol{a}_{\mathrm{CoM}_i}$ and ${}^i\dot{\boldsymbol{\omega}}_i$
    Compute ${}^i\boldsymbol{\mathcal{F}}^*_i$, ${}^i\boldsymbol{\mathcal{T}}^*_i$, ${}^i\boldsymbol{\pi}^*_i$, ${}^i\boldsymbol{\mathcal{F}}^g_i$, ${}^i\boldsymbol{\mathcal{F}}^s_i$, ${}^i\boldsymbol{\mathcal{T}}^s_i$ and ${}^i\boldsymbol{\pi}^s_i$
  end for
  for $i = N_B \to 1$ **do** ▷ Backward step
    Compute $\boldsymbol{Q}^a_j$ as given in (53) by using (40)–(41)
  end for

A. Gravitational force

The gravitational active force performing work on $\mathcal{B}_i$ is

$$ {}^i\boldsymbol{\mathcal{F}}^g_i = \int_{V_i} \boldsymbol{R}_i^T \boldsymbol{g} \mathrm{d}m_i = \boldsymbol{R}_i^T \boldsymbol{g} m_i = {}^i\boldsymbol{g} m_i, \tag{54} $$

being $\boldsymbol{g} \in \mathbb{R}^3$ the gravity vector in $\{S_0\}$ and ${}^i\boldsymbol{g}$ its representation in body coordinates. Similarly, we have

$$ {}^i\boldsymbol{\pi}^g_i = \nabla_{\dot{\boldsymbol{q}}_i} {}^i\dot{\boldsymbol{p}}_{\mathrm{CoM}_i} {}^i\boldsymbol{g} m_i. \tag{55} $$

The computation of ${}^i\boldsymbol{\mathcal{F}}^g_i$ can be performed sequentially from the first body to the last. By comparing (54) with (46) and (55) with (49), it is possible to see that the effect of gravity can be incorporated into the calculations by setting the acceleration of the base to ${}^0\boldsymbol{a}_0 = -\boldsymbol{g}$.

B. Interaction force

The derivation of the generalized interaction forces requires necessarily further hypotheses. Being undoubtedly the most used for control purposes, we assume a linear visco-elastic stress-strain relationship, so that $\boldsymbol{Q}^s_j = \boldsymbol{Q}^e_j + \boldsymbol{Q}^d_j$, and denote the corresponding forces (torques) as $\mathrm{d}{}^i\boldsymbol{f}^e_i$ ($\mathrm{d}{}^i\boldsymbol{\tau}^e_i$) and $\mathrm{d}{}^i\boldsymbol{f}^d_i$ ($\mathrm{d}{}^i\boldsymbol{\tau}^d_i$), respectively. Furthermore, let

$$ {}^i\boldsymbol{\mathcal{E}}_i = \boldsymbol{J}^T_{\boldsymbol{s}_i}({}^i\boldsymbol{r}_i)\boldsymbol{J}_{\boldsymbol{s}_i}({}^i\boldsymbol{r}_i) - \boldsymbol{J}^T_{\boldsymbol{s}_i}({}^i\boldsymbol{r}^*_i)\boldsymbol{J}_{\boldsymbol{s}_i}({}^i\boldsymbol{r}^*_i), $$

the Green-Lagrange strain tensor in the body coordinates, where ${}^i\boldsymbol{r}^*_i$ represents ${}^i\boldsymbol{r}_i$ in the reference configuration. According to the Hooke law, one has

$$ \mathrm{d}{}^i\boldsymbol{f}^e_i = \nabla_{\boldsymbol{s}_i} \cdot \left(2\mu_i {}^i\boldsymbol{\mathcal{E}}_i + \lambda_i \mathrm{tr}\left({}^i\boldsymbol{\mathcal{E}}_i\right)\boldsymbol{I}_3\right)\mathrm{d}V, $$

and

$$ \mathrm{d}{}^i\boldsymbol{\tau}^e_i = {}^i\boldsymbol{r}_i \times \mathrm{d}{}^i\boldsymbol{f}^e_i, $$

where $\lambda_i = \dfrac{E_i}{2(1+2\nu_i)}$ and $\mu_i = \dfrac{E_i\nu_i}{(1+\nu_i)(1-2\nu_i)}$ are the Lame constants of $\mathcal{B}_i$, with E_i and ν_i the material Young modulus and Poisson ratio, respectively. Note that the divergence operator projects the internal stress into the dynamic equations [51] . Similarly, considering a Kelvin–Voigt model for the viscous forces leads to

$$ \mathrm{d}{}^i\boldsymbol{f}^d_i = \eta_i \nabla_{\boldsymbol{s}_i} \cdot {}^i\dot{\boldsymbol{\mathcal{E}}}_i \mathrm{d}V, $$

and

$$ \mathrm{d}{}^i\boldsymbol{\tau}^d_i = {}^i\boldsymbol{r}_i \times \mathrm{d}{}^i\boldsymbol{f}^d_i, $$

being η_i the material viscosity. Finally, ${}^i\boldsymbol{\mathcal{F}}^s_i$, ${}^i\boldsymbol{\mathcal{T}}^s_i$ and ${}^i\boldsymbol{\pi}^s_i$ can be obtained by proper integration over the body as detailed in (33)– (34) and (37).

Remark 5. *More accurate models for the interaction forces can be considered. Indeed, from Property 1, a different model of these forces will affect only the computation of* $\boldsymbol{Q}^s_j$.

VI. Simulations

The main motivation of this work is to obtain a unified procedure to evaluate the GID and AID of serial modular mechanical systems for control purposes. In principle, this requires an experimental validation, which is out of scope given the theoretical nature of this paper and will be considered in future work. Nonetheless, we believe that a validation is helpful to show the generality of our approach. In this section, despite not being its main application, we exploit the AID algorithm to simulate new RoM for continuum soft robots.

Note: Additional simulation results on state of the art models can be found in the paper supplementary material at the following link: https://drive.google.com/drive/folders/13wwUjjX7jm1VkRfYzafbWKtey3qWZ1_a?usp=sharing.

In particular, Algorithm 2 is used to solve the FDP through the inertia-based algorithm [16], which we briefly summarize in the following. At each time step, the FDP requires solving the following linear system

$$ \boldsymbol{M}(\boldsymbol{q})\ddot{\boldsymbol{q}} = -\boldsymbol{n}(\boldsymbol{q}, \dot{\boldsymbol{q}}) + \boldsymbol{Q}(\boldsymbol{q}, \dot{\boldsymbol{q}}, \boldsymbol{u}). \tag{56} $$

Exploiting the linearity of the dynamics in the acceleration, the i-th column of $\boldsymbol{M}(\boldsymbol{q})$ can be computed calling the AID procedure as follows

$$ \boldsymbol{M}_i(\boldsymbol{q}) = \mathrm{AID}(\boldsymbol{q}, \boldsymbol{0}_n, (\boldsymbol{I}_n)_i). $$

Since the AID takes $O(N)$ computations, the cost to evaluate the mass matrix is $O(N^2)$. Similarly, the vectors appearing in the right-hand side of (56) can be computed by setting the acceleration to zero, i.e.,

$$ -\boldsymbol{n}(\boldsymbol{q}, \dot{\boldsymbol{q}}) + \boldsymbol{Q}(\boldsymbol{q}, \dot{\boldsymbol{q}}, \boldsymbol{u}) = \mathrm{GID}(\boldsymbol{q}, \dot{\boldsymbol{q}}, \boldsymbol{0}_n), $$

with a $O(N)$ computational cost. Observing that (56) requires solving a linear system of equations, the worst-case complexity for the computation of the FD with this approach is $O(N^3)$. Despite not being optimal, the possibility to simulate the dynamics with the ID comes for free without any further effort. In addition, the computation of $\boldsymbol{M}(\boldsymbol{q})$ can be parallelized, so improving the speed of the algorithm.

It is worth remarking that the same ID algorithm is used in all the following simulations. Every simulation is implemented by providing a different robot model to the procedure.

A. Simulation 1: PCC with variable radius

Consider a planar soft robot actuated with three pairs of antagonistic pneumatic chambers. Our method allows to easily model the effect of the chambers on the dynamics by introducing additional DoF for the radius change. To the best of our knowledge, this is the first time that such class of models is presented and simulated, and thus constitutes an additional contribution of this work. The kinematics is modeled by a combination of strain and radius configuration variables. The strain configuration encodes the pose of the robot backbone, while the radius variables model the shape alterations along the robot section. The continuum is discretized into three bodies with cylindrical shape in the stress free configuration, having each rest length $L_{0_i} = 0.2$ [m], radius $R_{0_i} = 0.02$ [m] and mass density $\rho_i = 1062$ $[\mathrm{kg\,m^{-3}}]; i = 1, 2$. The material visco-elastic parameters are $E_i = 1.06[\mathrm{MPa}]$, $\nu_i = 0.5$ and $\eta_i = 0.1$ [s]. The base is rotated so that in the straight configuration the robot is aligned with the gravitational field and points downwards. Each pneumatic chamber has a uniform distance $d_{c,i} = 0.004$ [m] from the body walls.

Each body $\mathcal{B}_i$ has in total four DoF. The first two model the curvature and elongation strains under the PCC hypothesis, i.e.,

$$\begin{pmatrix} \kappa_i(\boldsymbol{q}_i) \\ \delta L_i(\boldsymbol{q}_i) \end{pmatrix} = \frac{1}{L_{0_i}} \begin{pmatrix} 1 & 0 & 0 & 0 \\ 0 & 1 & 0 & 0 \end{pmatrix} \boldsymbol{q}_i + \begin{pmatrix} 0 \\ 1 \end{pmatrix}.$$

The remaining two configuration variables describe the change in radius R_i, namely

$$R_i(s_{i,2}, \boldsymbol{q}_i) = R_{0_i} + \delta R_i(s_{i,1}, s_{i,2}, \boldsymbol{q}_i),$$

where

$$\delta R_i = \begin{cases} \begin{pmatrix} 0 & 0 & b(s_{i,1}, s_{i,2}) & 0 \end{pmatrix} \boldsymbol{q}_i, & s_{i,1} \in [0, L_{0,i}], \; s_{i,2} \in [0, \pi); \\ \begin{pmatrix} 0 & 0 & 0 & b(s_{i,1}, s_{i,2} - \pi) \end{pmatrix} \boldsymbol{q}_i, & s_{i,1} \in [0, L_{0,i}], \; s_{i,2} \in [\pi, 2\pi); \\ \begin{pmatrix} 0 & 0 & 0 & 0 \end{pmatrix}, & \text{otherwise.} \end{cases},$$

models the radius change from R_{0_i}. The variable $s_{i,2}$ is used to locate for each cross section the pneumatic chamber. To model the functional dependence of δR_i on the material coordinates $s_{i,1}$ and $s_{i,2}$ we use the multivariate bump function

$$b(s_{i,1}, s_{i,2}) = e^{-\dfrac{L_{0_i}}{\frac{L_{0_i}^2}{4} - (s_{i,1} - \frac{L_{0_i}}{2})^2}} e^{-\dfrac{1}{\frac{\pi^2}{4} - (s_{i,2} - \frac{\pi}{2})^2}}.$$

This choice is motivated by empirical observation of pneumatically actuated soft robots, whose chamber deformation is usually larger at the middle of body.

The actuation generalized force $\boldsymbol{Q}_i^a(\boldsymbol{q}_i, \boldsymbol{u}_i)$ of $\mathcal{B}_i$ is modeled using the principle of virtual works leading to

$$\boldsymbol{Q}_i^a(\boldsymbol{q}_i, \boldsymbol{u}_i) = \nabla_{\boldsymbol{q}_i} \boldsymbol{V}_i(\boldsymbol{q}_i) \boldsymbol{u}_i, \tag{57}$$

where the vector $\boldsymbol{V}_i(\boldsymbol{q}_i) = \begin{pmatrix} V_{i,1}(\boldsymbol{q}_i) & V_{i,2}(\boldsymbol{q}_i) \end{pmatrix}^T$ collects the volume of the two pneumatic chambers in the current configuration and $\boldsymbol{u}_i = \begin{pmatrix} u_{i,1} & u_{i,2} \end{pmatrix}^T$ is the difference in chamber pressure with respect to the atmospheric pressure. The robot starts at rest from the stress free configuration $\boldsymbol{q}_0 = \boldsymbol{0}_{12}$ and the dynamics is excited with a constant input equal to

$$\boldsymbol{u} = \begin{pmatrix} 2 & 0 & 0 & 2 & 1 & 0.4 \end{pmatrix} [\mathrm{MPa}].$$

The volume integrals appearing in the ID algorithms and (57) are approximated using a Gaussian quadrature rule in spherical coordinates. Fig. 4 reports the time evolution of the configuration variables, divided into strain and radius variables, and a stroboscopic plot of the robot motion in its workspace.

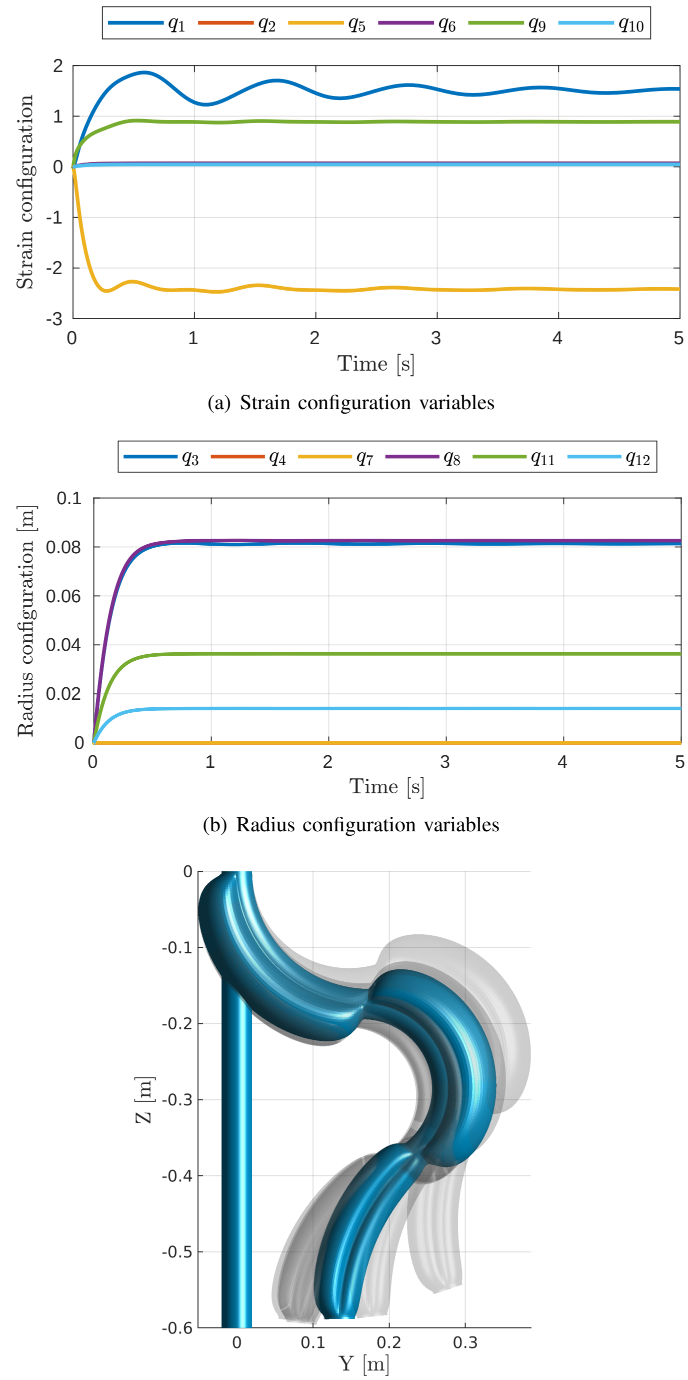

(a) Strain configuration variables

(b) Radius configuration variables

(c) Stroboscopic plot

Figure 4: Simulation 1: PCC with variable radius. Time evolution of the strain (a) and radius (b) configuration variables, and stroboscopic plot (c) for a planar soft arm with variable radius of three bodies and six pressure chambers. In (c), the initial and final configurations are depicted in blue, while the transient motion in light gray.

B. Simulation 2: PGC in free evolution

Consider a tentacle-like soft robotic arm of two bodies with conical shape. The first body has base and tip radius equal to $R_{\mathrm{base}_1} = 0.01$ [m] and $R_{\mathrm{tip}_1} = 0.005$ [m], respectively, while the second $R_{\mathrm{base}_2} = 0.005$ [m] and $R_{\mathrm{tip}_2} = 0.002$ [m]. The rest length and mass density are $L_{0_i} = 0.2$ [m] and

$\rho_i = 1070\,[\mathrm{kg/m^3}]$, respectively. The elastic parameters are $E_i = 0.666\,[\mathrm{GPa}]$ and $\nu_i = 0.4$, while the material viscosity is $\eta_i = 0.01\,[\mathrm{s}]; i = 1, 2$. The kinematics is computed using the Geometric Variable Strain approach of [53]. Inspired by [48], we model the strain using a Piecewise Gaussian Curvature (PGC) basis with elongation, defined as follows

$$\begin{pmatrix} \kappa_{x,i} \\ \kappa_{y,i} \\ \delta L_i \end{pmatrix} = \boldsymbol{\Phi}_i(s_i)\boldsymbol{q}_i + \begin{pmatrix} 0 \\ 0 \\ 1 \end{pmatrix},$$

where

$$\boldsymbol{\Phi}_i(s_i) = \frac{1}{L_{0_i}} \begin{pmatrix} 0 & 0 & -1 & -e^{-(s_i - L_{0_i}/2)^2} & 0 \\ 1 & e^{-(s_i - L_{0_i}/2)^2} & 0 & 0 & 0 \\ 0 & 0 & 0 & 0 & 1 \end{pmatrix},$$

$s_i \in [0, L_{0_i}]$ and $\boldsymbol{q}_i \in \mathbb{R}^5$. The robot starts at rest from the initial configuration

$$\boldsymbol{q}_0 = \begin{pmatrix} 0.3 & 1 & 0 & 1 & 0.1 & -1 & 0 & 0.1 & 2 & 0 \end{pmatrix}^T,$$

and the base is rotated so that in the stress-free configuration the arm is aligned with the gravitational field with the tip pointing upwards. The results of the simulation are shown in Fig. 5. After a transient of approximately 5 [s], the arm reaches a steady-state position consistent with the direction of the gravitational force.

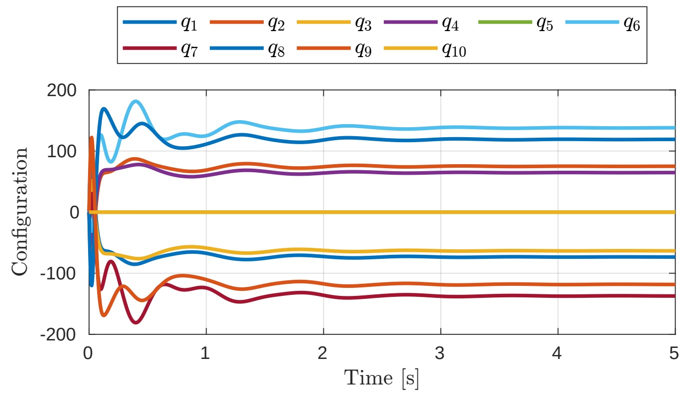

(a) Configuration variables

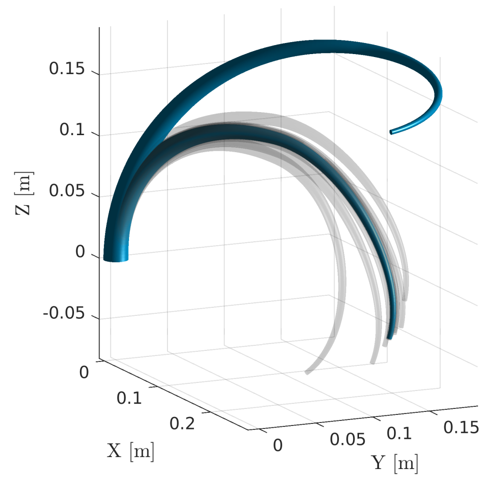

(b) Stroboscopic plot

Figure 5: Simulation 2: PGC in free evolution. Time evolution of the configuration variables (a) and stroboscopic plot (b) of a continuum soft robot modeled with a Gaussian model of the strain. In (b), the initial and final configurations are depicted in blue, while intermediate configurations in light gray.

VII. Conclusions and Future Work

This paper presents a recursive method for computing the inverse dynamics of serial mechanical systems assembled from complex modules. The procedure is general and independent of the body domain and type, meaning it can be used for a wide range of robots, including rigid and deformable bodies.

Considering an abstract kinematic model of each system module, the equations of motion are derived using the weak form of the dynamics and the Kane method. It is then proven that such equations admit a recursive expression, which allows for an efficient implementation of the inverse dynamics. The procedure has linear complexity in the number of bodies and is thus optimal. The versatility of the method is shown by simulating two novel reduced order models of continuum soft robots.

Future work will focus on the experimental validation of the method for synthesizing model-based controllers. We also aim to investigate how the algorithm must be modified to handle non-holonomic constraints. A further research direction is to use a similar approach to solve efficiently the forward dynamics problem.

Appendix

A. Proof of Proposition 2

To show the result it suffices to prove the equivalence between the Kane and Euler-Lagrange equations of a generic configuration variable q_k. To this end, consider the kinetic energy of the system

$$\mathcal{K} = \sum_{i=1}^{N} \mathcal{K}_i = \sum_{i=1}^{N} \int_{V_i} \frac{1}{2} \dot{\boldsymbol{p}}_i^T \dot{\boldsymbol{p}}_i \mathrm{d}m_i, \tag{58}$$

where $\mathcal{K}_i$ denotes the kinetic energy of $\mathcal{B}_i$. By the Reynolds transport theorem, it follows that

$$\begin{aligned} \frac{\mathrm{d}}{\mathrm{d}t}\left(\int_{V_i} \nabla_{q_k} \boldsymbol{p}_i^T \dot{\boldsymbol{p}}_i \mathrm{d}m_i\right) &= \int_{V_i} \frac{\mathrm{d}}{\mathrm{d}t}\left(\nabla_{q_k} \boldsymbol{p}_i^T \dot{\boldsymbol{p}}_i \mathrm{d}m_i\right) \\ &= \int_{V_i} \frac{\mathrm{d}}{\mathrm{d}t}\left(\nabla_{q_k} \boldsymbol{p}_i^T \dot{\boldsymbol{p}}_i\right) \mathrm{d}m_i, \end{aligned} \tag{59}$$

where in the last equality $\dot{\rho}_i = 0$ has been used. Expanding the derivative and rearranging the terms leads to

$$\begin{aligned} \int_{V_i} \nabla_{q_k} \boldsymbol{p}_i^T \ddot{\boldsymbol{p}}_i \mathrm{d}m_i = &\frac{\mathrm{d}}{\mathrm{d}t}\left(\int_{V_i} \nabla_{q_k} \boldsymbol{p}_i^T \dot{\boldsymbol{p}}_i \mathrm{d}m_i\right) \\ &- \int_{V_i} \frac{\mathrm{d}}{\mathrm{d}t}\left(\nabla_{q_k} \boldsymbol{p}_i^T\right) \dot{\boldsymbol{p}}_i \mathrm{d}m_i \end{aligned} \tag{60}$$

Now, note that

$$\int_{V_i} \nabla_{q_k} \boldsymbol{p}_i^T \dot{\boldsymbol{p}}_i \mathrm{d}m_i = \nabla_{\dot{q}_k} \int_{V_i} \frac{1}{2} \dot{\boldsymbol{p}}_i^T \dot{\boldsymbol{p}}_i \mathrm{d}m_i = \nabla_{\dot{q}_k} \mathcal{K}_i,$$

and

$$\int_{V_i} \nabla_{q_k} \dot{\boldsymbol{p}}_i^T \dot{\boldsymbol{p}}_i \mathrm{d}m_i = \nabla_{q_k} \int_{V_i} \frac{1}{2} \dot{\boldsymbol{p}}_i^T \dot{\boldsymbol{p}}_i \mathrm{d}m_i = \nabla_{q_k} \mathcal{K}_i,$$

which substituted in (60) yields

$$\int_{V_i} \nabla_{q_k} \boldsymbol{p}_i^T \ddot{\boldsymbol{p}}_i \mathrm{d}m_i = \frac{\mathrm{d}}{\mathrm{d}t} \left(\nabla_{\dot{q}_k} \mathcal{K}_i \right) - \nabla_{q_k} \mathcal{K}_i.$$

By exploiting the linearity of the differentiation, one has

$$\begin{aligned} \sum_{i=1}^{N} \int_{V_i} \nabla_{q_k} \boldsymbol{p}_i^T \ddot{\boldsymbol{p}}_i \mathrm{d}m_i &= \sum_{i=1}^{N} \frac{\mathrm{d}}{\mathrm{d}t} \left(\nabla_{\dot{q}_k} \mathcal{K}_i \right) - \nabla_{q_k} \mathcal{K}_i \\ &= \frac{\mathrm{d}}{\mathrm{d}t} \left(\nabla_{\dot{q}_k} \sum_{i=1}^{N} \mathcal{K}_i \right) - \nabla_{q_k} \sum_{i=1}^{N} \mathcal{K}_i \\ &= \frac{\mathrm{d}}{\mathrm{d}t} \left(\nabla_{\dot{q}_k} \mathcal{K} \right) - \nabla_{q_k} \mathcal{K} \end{aligned}$$

Replacing the above equation in (23) finally gives

$$Q_k = \frac{\mathrm{d}}{\mathrm{d}t} \left(\nabla_{\dot{q}_k} \mathcal{K} \right) - \nabla_{q_k} \mathcal{K}.$$

The result follows by recalling that $Q_k = -Q_k^*$ and observing that the right-hand side of the above equations is the k-th row of (1).

B. Proof of Theorem 1

In the following, we prove that (40)–(41) is a recursive expression of $\boldsymbol{\mathcal{M}}_j$ as defined in (39). First, note that, for all $i \geq j$, the following identities hold

$$\begin{aligned} \nabla_{\dot{\boldsymbol{q}}_j} {}^{i+1}\boldsymbol{v}_{i+1} = \nabla_{\dot{\boldsymbol{q}}_j} {}^{i}\boldsymbol{v}_i {}^{i}\boldsymbol{R}_{i+1} \\ + \nabla_{\dot{\boldsymbol{q}}_j} {}^{i}\boldsymbol{\omega}_i {}^{i}\boldsymbol{t}_{i+1} \times {}^{i}\boldsymbol{R}_{i+1}, \end{aligned} \tag{61}$$

$$\nabla_{\dot{\boldsymbol{q}}_j} {}^{i+1}\boldsymbol{\omega}_{i+1} = \nabla_{\dot{\boldsymbol{q}}_j} {}^{i}\boldsymbol{\omega}_i {}^{i}\boldsymbol{R}_{i+1}. \tag{62}$$

The result follows by iteratively exploiting the above equations. In particular, consider the right-hand side of (40), repeated below for the ease of readability

$$\nabla_{\dot{\boldsymbol{q}}_j} {}^{j}\boldsymbol{v}_j \left({}^{j}\boldsymbol{F}_j + {}^{j}\boldsymbol{F}_j^* \right) + \nabla_{\dot{\boldsymbol{q}}_j} {}^{j}\boldsymbol{\omega}_j \left({}^{j}\boldsymbol{T}_j + {}^{j}\boldsymbol{T}_j^* \right). \tag{63}$$

Replacing (41) into the previous equation gives

$$\begin{aligned} &\nabla_{\dot{\boldsymbol{q}}_j} {}^{j}\boldsymbol{v}_j \left({}^{j}\boldsymbol{F}_j + {}^{j}\boldsymbol{F}_j^* \right) + \nabla_{\dot{\boldsymbol{q}}_j} {}^{j}\boldsymbol{\omega}_j \left({}^{j}\boldsymbol{T}_j + {}^{j}\boldsymbol{T}_j^* \right) \\ &= \nabla_{\dot{\boldsymbol{q}}_j} {}^{j}\boldsymbol{v}_j \left({}^{j}\boldsymbol{\mathcal{F}}_j + {}^{j}\boldsymbol{\mathcal{F}}_j^* \right) + \nabla_{\dot{\boldsymbol{q}}_j} {}^{j}\boldsymbol{\omega}_j \\ &\qquad \left({}^{j}\boldsymbol{\mathcal{T}}_j + {}^{j}\boldsymbol{\mathcal{T}}_j^* + {}^{j}\boldsymbol{p}_{\mathrm{CoM}_j} \times \left({}^{j}\boldsymbol{\mathcal{F}}_j + {}^{j}\boldsymbol{\mathcal{F}}_j^* \right) \right) \\ &\quad + \nabla_{\dot{\boldsymbol{q}}_j} {}^{j}\boldsymbol{v}_j {}^{j}\boldsymbol{R}_{j+1} \left({}^{j+1}\boldsymbol{F}_{j+1} + {}^{j+1}\boldsymbol{F}_{j+1}^* \right) \\ &\quad + \nabla_{\dot{\boldsymbol{q}}_j} {}^{j}\boldsymbol{\omega}_j {}^{j}\boldsymbol{R}_{j+1} \left({}^{j+1}\boldsymbol{T}_{j+1} + {}^{j+1}\boldsymbol{T}_{j+1}^* \right) \\ &\quad + \nabla_{\dot{\boldsymbol{q}}_j} {}^{j}\boldsymbol{\omega}_j {}^{j}\boldsymbol{t}_{j+1} \times {}^{j}\boldsymbol{R}_{j+1} \left({}^{j+1}\boldsymbol{F}_{j+1} + {}^{j+1}\boldsymbol{F}_{j+1}^* \right). \end{aligned}$$

By direct inspection, one can recognize that the first two terms of the above equation correspond to the first two in the expanded right-hand side of (39). On the other hand, the remaining three elements have the same form of the right-hand side of (61) or (62), which can be exploited to obtain

$$\begin{aligned} &\nabla_{\dot{\boldsymbol{q}}_j} {}^{j}\boldsymbol{v}_j \left({}^{j}\boldsymbol{F}_j + {}^{j}\boldsymbol{F}_j^* \right) + \nabla_{\dot{\boldsymbol{q}}_j} {}^{j}\boldsymbol{\omega}_j \left({}^{j}\boldsymbol{T}_j + {}^{j}\boldsymbol{T}_j^* \right) \\ &= \nabla_{\dot{\boldsymbol{q}}_j} {}^{j}\boldsymbol{v}_j \left({}^{j}\boldsymbol{\mathcal{F}}_j + {}^{j}\boldsymbol{\mathcal{F}}_j^* \right) \\ &+ \nabla_{\dot{\boldsymbol{q}}_j} {}^{j}\boldsymbol{\omega}_j \left({}^{j}\boldsymbol{\mathcal{T}}_j + {}^{j}\boldsymbol{\mathcal{T}}_j^* + {}^{j}\boldsymbol{p}_{\mathrm{CoM}_j} \times \left({}^{j}\boldsymbol{\mathcal{F}}_j + {}^{j}\boldsymbol{\mathcal{F}}_j^* \right) \right) \\ &+ \nabla_{\dot{\boldsymbol{q}}_j} {}^{j+1}\boldsymbol{v}_{j+1} \left({}^{j+1}\boldsymbol{F}_{j+1} + {}^{j+1}\boldsymbol{F}_{j+1}^* \right) \\ &+ \nabla_{\dot{\boldsymbol{q}}_j} {}^{j+1}\boldsymbol{\omega}_{j+1} \left({}^{j+1}\boldsymbol{T}_{j+1} + {}^{j+1}\boldsymbol{T}_{j+1}^* \right). \end{aligned} \tag{64}$$

The last two terms of (64) have again the same form of (63) but with increased index. The result follows by repeating the last two steps until the N-th term appears.

REFERENCES

[1] S. Lee, S. Noh, Y. Lee, and J. H. Park, "Development of bio-mimetic robot hand using parallel mechanisms," in *IEEE Int. Conf. on Robotics and Biomimetics*, 2009, pp. 550–555.

[2] A. De Luca and W. J. Book, "Robots with flexible elements," in *Springer Handbook of Robotics*, B. Siciliano and O. Khatib, Eds. Springer, 2016, pp. 243–282.

[3] F. Hu, W. Wang, J. Cheng, and Y. Bao, "Origami spring–inspired metamaterials and robots: An attempt at fully programmable robotics," *Science Progress*, vol. 103, no. 3, p. 0036850420946162, 2020.

[4] D. Bevilacqua, G. Soleti, D. Naso, G. Rizzello, and P. Motzki, "Bio-inspired flapping wing antagonist actuation with SMA wires," in *Int. Conf. and Exhibition on New Actuator Systems and Applications*, 2022, pp. 1–4.

[5] D. Rus and M. T. Tolley, "Design, fabrication and control of soft robots," *Nature*, vol. 521, no. 7553, pp. 467–475, 2015.

[6] M. Russo, S. M. H. Sadati, X. Dong, A. Mohammad, I. D. Walker, C. Bergeles, K. Xu, and D. A. Axinte, "Continuum robots: An overview," *Advanced Intelligent Systems*, vol. 5, no. 5, p. 2200367, 2023.

[7] H. Yin, A. Varava, and D. Kragic, "Modeling, learning, perception, and control methods for deformable object manipulation," *Science Robotics*, vol. 6, no. 54, p. eabd8803, 2021.

[8] H. W. M. Hoeijmakers, L. H. G. Koerkamp, L. D. de Santana, C. H. Venner, S. Stramigioli, J. L. Mulder, A. Brentjes, F. Gijsman, and S. A. Hartman, "Investigation flapping-flight aerodynamics of a robotic bird," in *Proc. 33th Congress of the Int. Council of the Aeronautical Sciences*, 2022, pp. 3326–3351.

[9] T.-W. Liu, J.-B. Bai, S.-L. Li, and N. Fantuzzi, "Large deformation and failure analysis of the corrugated flexible composite skin for morphing wing," *Engineering Structures*, vol. 278, p. 115463, 2023.

[10] L. Sun, Y. Yu, Z. Chen, F. Bian, F. Ye, L. Sun, and Y. Zhao, "Biohybrid robotics with living cell actuation," *Chemical Society Reviews*, vol. 49, no. 12, pp. 4043–4069, 2020.

[11] B. Wang, K. F. Chan, K. Yuan, Q. Wang, X. Xia, L. Yang, H. Ko, Y.-X. J. Wang, J. J. Y. Sung, P. W. Y. Chiu, and L. Zhang, "Endoscopy-assisted magnetic navigation of biohybrid soft microrobots with rapid endoluminal delivery and imaging," *Science Robotics*, vol. 6, no. 52, p. eabd2813, 2021.

[12] Z. Lin, T. Jiang, and J. Shang, "The emerging technology of biohybrid micro-robots: A review," *Bio-Design and Manufacturing*, pp. 1–26, 2022.

[13] J. Zhu, A. Cherubini, C. Dune, D. Navarro-Alarcon, F. Alambeigi, D. Berenson, F. Ficuciello, K. Harada, J. Kober, X. Li, J. Pan, W. Yuan, and M. Gienger, "Challenges and outlook in robotic manipulation of deformable objects," *IEEE Robotics & Automation Mag.*, vol. 29, no. 3, pp. 67–77, 2022.

[14] B. Vanderborght, A. Albu-Schaeffer, A. Bicchi, E. Burdet, D. Caldwell, R. Carloni, M. Catalano, O. Eiberger, W. Friedl, G. Ganesh, M. Garabini, M. Grebenstein, G. Grioli, S. Haddadin, H. Hoppner, A. Jafari, M. Laffranchi, D. Lefeber, F. Petit, S. Stramigioli, N. Tsagarakis, M. Van Damme, R. Van Ham, L. Visser, and S. Wolf, "Variable impedance actuators: A review," *Robotics and Autonomous Systems*, vol. 61, no. 12, pp. 1601–1614, 2013.

[15] C. Della Santina, M. G. Catalano, and A. Bicchi, "Soft robots," in *Encyclopedia of Robotics*, M. Ang, O. Khatib, and B. Siciliano, Eds. Springer, 2020, pp. 1–15.

[16] R. Featherstone, *Rigid Body Dynamics Algorithms*. Springer, 2014.

[17] A. A. Shabana, "Flexible multibody dynamics: Review of past and recent developments," *Multibody System Dynamics*, vol. 1, pp. 189–222, 1997.

[18] S. F. Dehkordi, "Dynamic analysis of flexible-link manipulator in underwater applications using Gibbs-Appell formulations," *Ocean Engineering*, vol. 241, p. 110057, 2021.

[19] A. Zwölfer and J. Gerstmayr, "A unified framework for corotational flexible multibody system dynamics formulations." *J. of Structural Dynamics*, vol. 2, pp. 51–81, 2023.

[20] F. Renda, F. Boyer, J. Dias, and L. Seneviratne, "Discrete Cosserat approach for multisection soft manipulator dynamics," *IEEE Trans. on Robotics*, vol. 34, no. 6, pp. 1518–1533, 2018.

[21] D. Dinev, T. Liu, J. Li, B. Thomaszewski, and L. Kavan, "FEPR: Fast energy projection for real-time simulation of deformable objects," *ACM Trans. on Graphics*, vol. 37, no. 4, pp. 1–12, 2018.

[22] S. Grazioso, G. Di Gironimo, and B. Siciliano, "A geometrically exact model for soft continuum robots: The finite element deformation space formulation," *Soft Robotics*, vol. 6, no. 6, pp. 790–811, 2019.

[23] F. Boyer, V. Lebastard, F. Candelier, and F. Renda, "Dynamics of continuum and soft robots: A strain parameterization based approach," *IEEE Trans. on Robotics*, vol. 37, no. 3, pp. 847–863, 2020.

[24] G. Buondonno and A. De Luca, "Efficient computation of inverse dynamics and feedback linearization for VSA-based robots," *IEEE Robotics and Automation Lett.*, vol. 1, no. 2, pp. 908–915, 2016.

[25] Y. Liu, T. Li, J. Duan, X. Wu, H. Wang, Q. Fan, J. Lin, and Y. Hu, "On a hierarchical adaptive and robust inverse dynamic control strategy with experiment for robot manipulators under uncertainties," *Control Engineering Practice*, vol. 138, p. 105604, 2023.

[26] C. Gaz, M. Cognetti, A. Oliva, P. Robuffo Giordano, and A. De Luca, "Dynamic identification of the Franka Emika Panda robot with retrieval of feasible parameters using penalty-based optimization," *IEEE Robotics and Automation Lett.*, vol. 4, no. 4, pp. 4147–4154, 2019.

[27] A. Longhini, M. Moletta, A. Reichlin, M. C. Welle, D. Held, Z. Erickson, and D. Kragic, "Edo-net: Learning elastic properties of deformable objects from graph dynamics," in *Proc. IEEE Int. Conf. on Robotics and Automation*, 2023, pp. 3875–3881.

[28] F. Saunders, B. A. Trimmer, and J. Rife, "Modeling locomotion of a soft-bodied arthropod using inverse dynamics," *Bioinspiration & Biomimetics*, vol. 6, no. 1, p. 016001, 2010.

[29] H. Ferrolho, V. Ivan, W. Merkt, I. Havoutis, and S. Vijayakumar, "Inverse dynamics vs. forward dynamics in direct transcription formulations for trajectory optimization," in *Proc. IEEE Int. Conf. on Robotics and Automation*, 2021, pp. 12 752–12 758.

[30] F. Chen and M. Y. Wang, "Design optimization of soft robots: A review of the state of the art," *IEEE Robotics & Automation Mag.*, vol. 27, no. 4, pp. 27–43, 2020.

[31] J. Pinskier and D. Howard, "From bioinspiration to computer generation: Developments in autonomous soft robot design," *Advanced Intelligent Systems*, vol. 4, no. 1, p. 2100086, 2022.

[32] W. J. Book, "Recursive Lagrangian dynamics of flexible manipulator arms," *Int. Journal of Robotics Research*, vol. 3, no. 3, pp. 87–101, 1984.

[33] W. Chen, "Dynamic modeling of multi-link flexible robotic manipulators," *Computers & Structures*, vol. 79, no. 2, pp. 183–195, 2001.

[34] D.-g. Zhang, "Recursive Lagrangian dynamic modeling and simulation of multi-link spatial flexible manipulator arms," *Applied Mathematics and Mechanics*, vol. 30, no. 10, pp. 1283–1294, 2009.

[35] C. A. My, D. X. Bien, C. H. Le, and M. Packianather, "An efficient finite element formulation of dynamics for a flexible robot with different type of joints," *Mechanism and Machine Theory*, vol. 134, pp. 267–288, 2019.

[36] A. A. Shabana, "Dynamics of flexible bodies using generalized Newton-Euler equations," *J. of Dynamic Systems, Measurement, and Control*, vol. 112, no. 3, pp. 496–503, 1990.

[37] F. Boyer and W. Khalil, "An efficient calculation of flexible manipulator inverse dynamics," *Int. Journal of Robotics Research*, vol. 17, no. 3, pp. 282–293, 1998.

[38] W. Khalil, F. Boyer, and F. Morsli, "General dynamic algorithm for floating base tree structure robots with flexible joints and links," *J. of Mechanisms and Robotics*, vol. 9, no. 3, p. 031003, 2017.

[39] M. H. Korayem, A. M. Shafei, and S. F. Dehkordi, "Systematic modeling of a chain of n-flexible link manipulators connected by revolute–prismatic joints using recursive Gibbs-Appell formulation," *Archive of Applied Mechanics*, vol. 84, pp. 187–206, 2014.

[40] R. P. Singh, R. J. VanderVoort, and P. W. Likins, "Dynamics of flexible bodies in tree topology – A computer-oriented approach," *J. of Guidance, Control, and Dynamics*, vol. 8, no. 5, pp. 584–590, 1985.

[41] A. K. Banerjee and J. M. Dickens, "Dynamics of an arbitrary flexible body in large rotation and translation," *J. of Guidance, Control, and Dynamics*, vol. 13, no. 2, pp. 221–227, 1990.

[42] F. M. L. Amirouche and M. Xie, "An explicit matrix formulation of the dynamical equations for flexible multibody systems: A recursive approach," *Computers & Structures*, vol. 46, no. 2, pp. 311–321, 1993.

[43] F. Renda and L. Seneviratne, "A geometric and unified approach for modeling soft-rigid multi-body systems with lumped and distributed degrees of freedom," in *Proc. IEEE Int. Conf. on Robotics and Automation*, 2018, pp. 1567–1574.

[44] Y. Xu and G. S. Chirikjian, "Model reduction in soft robotics using locally volume-preserving primitives," *IEEE Robotics and Automation Lett.*, vol. 8, no. 9, pp. 5831–5838, 2023.

[45] T. R. Kane and D. A. Levinson, "The use of Kane's dynamical equations in robotics," *Int. J. of Robotics Research*, vol. 2, no. 3, pp. 3–21, 1983.

[46] A. Banerjee, *Flexible Multibody Dynamics: Efficient Formulations with Applications*, 2nd ed. CRC Press, 2022.

[47] J. M. Hollerbach, "A recursive Lagrangian formulation of maniputator dynamics and a comparative study of dynamics formulation complexity," *IEEE Trans. on Systems, Man, and Cybernetics*, vol. 10, no. 11, pp. 730–736, 1980.

[48] T. Wang, U. Halder, E. Gribkova, M. Gazzola, and P. G. Mehta, "Control-oriented modeling of bend propagation in an octopus arm," in *2022 American Control Conf.*, 2022, pp. 1359–1366.

[49] P. Pustina, C. Della Santina, and A. De Luca, "Universal inverse dynamics for multibody systems via Kane equations: Supplementary material," https://.

[50] C. Della Santina, A. Bicchi, and D. Rus, "On an improved state parametrization for soft robots with piecewise constant curvature and its use in model based control," *IEEE Robotics and Automation Lett.*, vol. 5, no. 2, pp. 1001–1008, 2020.

[51] W. Lacarbonara, *Nonlinear Structural Mechanics: Theory, Dynamical Phenomena and Modeling*. Springer, 2013.

[52] P. J. Davis and P. Rabinowitz, *Methods of numerical integration*. Courier Corporation, 2007.

[53] F. Renda, C. Armanini, V. Lebastard, F. Candelier, and F. Boyer, "A geometric variable-strain approach for static modeling of soft manipulators with tendon and fluidic actuation," *IEEE Robotics and Automation Lett.*, vol. 5, no. 3, pp. 4006–4013, 2020.